

# On the resolution of categorical symmetries in (Non-) Unitary Rational CFTs

---

**Arpan Bhattacharyya, Saptaswa Ghosh, Sounak Pal, Jagannath Santara**

*Department of Physics, Indian Institute of Technology, Gandhinagar, Gujarat-382055, India*

*E-mail:* [abhattacharyya@iitgn.ac.in](mailto:abhattacharyya@iitgn.ac.in), [saptaswaghosh@iitgn.ac.in](mailto:saptaswaghosh@iitgn.ac.in),  
[palsounak@iitgn.ac.in](mailto:palsounak@iitgn.ac.in), [jagannath.santara@iitgn.ac.in](mailto:jagannath.santara@iitgn.ac.in)

**ABSTRACT:** We explore several aspects of the categorical symmetry-resolved entanglement entropy (SREE) in two-dimensional Rational Conformal Field Theories (RCFTs) and express it directly in terms of the modular data of the theory. Motivated by [1], we provide a general formula for SREE that applies to symmetric (weakly/strongly) and cloaking boundary conditions as well as for fusion rings with multiplicities without invoking any SymTFT construction, relying instead on a purely 2d RCFT analysis. We check the formula against several explicit examples. Additionally, we study symmetry resolution for both categorical and invertible symmetries in (non-)diagonal RCFTs and comment on the subtleties that arise in these cases. Finally, we extend our analysis to diagonal non-unitary RCFTs, focusing on theories with generalized Haagerup–Izumi modular data, and find full agreement with the given formula.

---

## Contents

<b>1</b>	<b>Introduction</b>	<b>1</b>
<b>2</b>	<b>Background and basic setup</b>	<b>5</b>
<b>3</b>	<b>Symmetry resolved entanglement entropy (SREE)</b>	<b>8</b>
<b>4</b>	<b>Computing SREE in Unitary Rational CFT</b>	<b>13</b>
4.1	Symmetry resolution with respect to Tambara-Yamagami (TY) Fusion Category for Ising CFT	13
4.2	Symmetry resolution for $\mathcal{M}(6, 5)$	15
4.3	Symmetry resolution in non-diagonal RCFTs	18
<b>5</b>	<b>SREE in Non-Unitary Rational CFT</b>	<b>21</b>
5.1	Lee-Yang Minimal Model $\mathcal{M}(5, 2)$ : a simplest example	22
5.2	The Haagerup Rational CFT $\mathcal{R}_{\kappa=3}$	24
5.3	The Haagerup Rational CFT $\mathcal{R}_{\kappa=4}$	26
5.4	The Haagerup Rational CFT $\mathcal{R}_{\kappa=5}$	29
<b>6</b>	<b>Summary and Conclusion</b>	<b>31</b>
<b>A</b>	<b>Another non-unitary minimal model <math>\mathcal{M}(7, 2)</math></b>	<b>33</b>

---

## 1 Introduction

Symmetries are omnipresent in nature. In physics, symmetry plays a crucial role in understanding the dynamics of quantum field theory and provides a framework for going beyond. According to Wigner [2], each symmetry is associated with a unitary operation that has an inverse, i.e., group-like. Gaiotto et al. [3] showed that the generalized global symmetry of a theory is associated with a topological defect operator, and there are plenty of examples found in condensed matter systems that realize this generalized global symmetry [4]. One of the classes of these generalized symmetries is famously known as *non-invertible symmetry* [5–32]<sup>1</sup>, which can not be described by a unitary operation, more specifically, it does not have an inverse. In mathematics literature, it is known as a category [33, 34]. For these kinds

---

<sup>1</sup>The references mentioned here are by no means exhaustive. Interested readers are referred to some of these reviews and lecture notes and their citations [4, 17, 19] for more references.

of categorical (non-invertible) symmetries, associated topological operators  $\{\mathcal{L}_a\}$  obey fusion rules of a tensor category rather than a group law, as shown below,

$$\mathcal{L}_a \times \mathcal{L}_b = \bigoplus_c \mathcal{N}_{ab}^c \mathcal{L}_c \quad (1.1)$$

where,  $\mathcal{N}_{ab}^c \in \mathbb{Z}_{\geq 0}$  is the fusion coefficients. These defect lines usually do not have a formal inverse, i.e., there exists no  $\mathcal{L}^{-1}$  such that  $\mathcal{L} \times \mathcal{L}^{-1} = \mathbb{I}$ .

There are numerous examples that demonstrate this kind of *categorical* symmetry exists in various branches of physics, including high-energy theory, mathematical physics, and condensed matter physics, particularly in low-dimensional quantum systems that are useful for quantum computation [4, 35–49]. Before delving into the main discussion of the paper regarding the categorical symmetry resolution of the entanglement entropy, we briefly discuss the representation of categories and the importance of dealing with the Drinfeld centre or the quantum double  $Z(\mathcal{C})$  of a given category  $\mathcal{C}$ .

**Fusion category and tube algebra.** As discussed above, the symmetry operations will be encoded by a fusion (tensor) category  $\mathcal{C}$  generated by topological lines  $\{\mathcal{L}_a\}$ . While  $\mathcal{C}$  is not itself an algebra, one can canonically associate a tube algebra to it using the construction of Ocneanu [50] as follows. Consider an annulus (“tube”) whose inner and outer boundaries are labeled by  $i, j \in \text{Irr}(\mathcal{C})$  and with a line  $x \in \text{Irr}(\mathcal{C})$  running along the tube’s axis. Stacking such tubes and recoupling via  $F$ -moves defines a product on the space

$$\text{Tube}(\mathcal{C}) = \bigoplus_{x,i,j \in \text{Irr}(\mathcal{C})} \text{Hom}_{\mathcal{C}}(i \otimes x, x \otimes j), \quad (1.2)$$

making it a finite-dimensional  $*$ -algebra; the involution is given by orientation reversal (Hermitian adjoint on morphisms). There is a canonical equivalence [51, 52]

$$\text{Rep}(\text{Tube}(\mathcal{C})) \simeq Z(\mathcal{C}). \quad (1.3)$$

Therefore, simple  $\text{Tube}(\mathcal{C})$ -modules are in one-to-one correspondence with the simple objects (the “anyon types”) of the Drinfeld center  $Z(\mathcal{C})$ . In other words, the irreducible representations of  $\text{Tube}(\mathcal{C})$  are canonically identified with the simple topological defect lines of  $Z(\mathcal{C})$ , and each representation is characterized by the quantum dimension of the corresponding simple object. Consequently, for a quantum system whose categorical symmetry is described by a semisimple fusion category  $\mathcal{C}$ , the analysis of its symmetry sectors is naturally equivalent to studying the symmetry sectors of the Drinfeld center  $Z(\mathcal{C})$ .

**Categorical symmetry-resolved entanglement.** Parallel to recent advances in the characterization of (non-)invertible symmetries, a complementary line of research has focused on the role of symmetries in shaping entanglement structures in quantum field theories (QFTs). Entanglement serves as a fundamental measure of quantum correlations and phases of matter, and provides a particularly sensitive probe of underlying symmetry principles, including generalized and non-invertible symmetries. In this context, symmetry-resolved entanglement

entropy (SREE) [53–75]<sup>2</sup> has emerged as a refined diagnostic that decomposes the total entanglement into contributions associated with individual symmetry sectors, thereby elucidating how symmetry structures govern the distribution of quantum information. Recent developments further demonstrate that non-invertible symmetries can impose nontrivial constraints on entanglement patterns, influence topological order, and enforce selection rules that transcend those encountered in the setting of ordinary invertible symmetries [77–80]. Motivated by these developments, this paper examines how non-invertible (categorical) symmetries modify entanglement measures in certain two-dimensional topological systems at criticality. For global invertible symmetries, SREE has been extensively studied, allowing the entanglement to be resolved sector by sector. Readers are referred to these reviews [76]. In contrast, symmetry resolution for *categorical* symmetries [1, 81–85] remains far less explored. In (1+1)-dimensional CFTs with a categorical symmetry encoded by a fusion category  $\mathcal{C}$ , symmetry resolution can be formulated in terms of boundary CFT (BCFT) [69, 72, 73] through projections onto categorical sectors. These projections are implemented by *symmetric* (either strongly or weakly) boundary states on which the corresponding topological defect lines can end. Now, on the replica geometry [86], inserting compatible defect endpoints along the branch cut yields well-defined sector probabilities and sector-resolved Rényi and von Neumann entropies. This construction is valid whenever the categorical symmetry is non-anomalous, i.e. free of obstructions to gauging [87, 88]. Alternatively, there is a twist-field approach that compute directly symmetry-resolved entanglement entropy using charged moments and this method is applied to compute SREE for rational CFT with Lie group symmetry by [89] and for certain non-invertible [85].

Interestingly, for 2d CFTs with global internal abelian symmetry, SREE shows universal results in the sense of *equipartition of entanglement* among all charge sector [54, 76]<sup>3</sup>. On the other hand, in the context of rational CFTs (RCFTs)<sup>4</sup>, for non-invertible categorical symmetry-resolved entanglement entropy, this equipartition of the entanglement is broken [72]. These deviations are controlled by the fusion data of  $\mathcal{C}$  and by the choice of symmetric boundary condition. Note that computation of the entanglement requires partitioning the Hilbert space, hence the boundary state placed at the entangling surface plays a crucial role in refining the entropy [91, 92]. In contrast to the group-like setting, non-invertible symmetries generally admit multiple, and often inequivalent, choices of boundary conditions. Although this issue has been noted in the literature [1, 78, 83, 84, 87, 93], previous discussions have largely centered on the so-called weakly/strongly symmetric boundary condition and with a multiplicity-free fusion ring. In this work, we revisit this question through a series of concrete examples that clarify how different boundary conditions naturally arise and how they affect the symmetry resolution. In particular, we highlight situations in which the weakly symmetric

---

<sup>2</sup>For more references and details, interested readers are referred to the following review of symmetry-resolved entanglement measure [76].

<sup>3</sup>One may note that for abelian symmetry the entanglement equipartition does not hold for all order of UV cutoff, see [73, 90].

<sup>4</sup>It turns out that almost all rational CFTs possess non-invertible symmetry.

boundary state is absent and motivate the use of cloaking boundary conditions (or states) [94, 95], which, despite not corresponding to physical Cardy states, play a crucial role in implementing symmetry resolution in non-invertible symmetries consistently.

**Non-unitarity and symmetry resolution.** Most developments on symmetry resolution have focused on *unitary* settings, where the physical Hilbert space and defect operations admit a positive-definite inner product, with positive central charge. In contrast, symmetry resolution for categorical symmetries in non-unitary setting remains comparatively unexplored, despite clear motivation [96, 97]. By the bulk–boundary correspondence, when a (2+1)-dimensional topological phase is described by a unitary TQFT, the universal properties of its gapless boundary are captured by a two-dimensional unitary RCFT [98–103]. Extending this logic beyond unitarity is natural [104]. It has been argued that a family of *non-unitary* TQFTs arises from topological twists of certain three-dimensional  $\mathcal{N} = 4$  rank-zero (S-fold) SCFTs, producing modular data that generalize the *non-unitary Haagerup–Izumi modular data* [105, 106]. This, in turn, leads to the question of whether there exist boundary RCFTs compatible with such generalized Haagerup modular data [107, 108]. The answer is affirmative: using the so-called Riemann–Hilbert approach, conformal characters consistent with the proposed modular data have been explicitly constructed [105]. These developments supply a concrete arena in which to formulate and study *categorical symmetry resolved entanglement* for non-unitary RCFTs, thereby extending symmetry resolution beyond the unitary paradigm. At this point, note that there are recent studies aimed at constructing critical lattice models in two dimensions, realizing the symmetry associated with the *unitary* Haagerup fusion category  $H_3$  [109–112] and extracted the central charge (and operator spectra) which turns out to be  $c \sim 2$ . Then it was further conjectured that this two-dimensional CFT can be constructed by a taking coset of a Haagerup rational CFT characterized central charge multiple of 8 [108], even though there is a puzzle regarding the existence of such  $c = 8$  unitary rational CFT with Haagerup fusion  $\mathcal{Z}(H_3)$  (for more details, interested readers are referred to T. Gannon’s talk [113])<sup>5</sup>. Nonetheless, we draw motivations from these studies and focus on certain non-unitary generalized Haagerup fusion categories [105] (some of them are tensor products of certain non-unitary minimal models) and discuss symmetry-resolution of entanglement entropy.

**Goal and brief takeaway.** *Besides the mentioned developments in the computation of SREE, the resolution in non-diagonal and non-unitary theories remains immensely unexplored. In this paper, we intend to fill this gap. This paper aims to bridge this gap by extending the analysis of categorical symmetry resolution to the domains of non-diagonal and non-unitary RCFTs.* We provide a general computational framework for computing the SREE in these theories, expressing it directly in terms of their modular data. Our work provides a unified framework that encompasses a wide range of scenarios, including different types of boundary conditions and fusion rings with multiplicities. We test the general formula against

---

<sup>5</sup>Recently, entanglement asymmetry for  $\mathcal{Z}(H_3)$  has been computed [114].

several explicit examples, including unitary diagonal models such as Ising CFT, tetracritical Ising CFT, and non-unitary models realized by *generalized* Haagerup-Izumi modular data. We also make comments on the subtleties and limitations of BCFT techniques while applied to non-diagonal theories with the example of non-diagonal  $SU(2)_{10}$  type  $E_6$ , and its  $\frac{1}{2}E_6$  resolution.

Our paper is organised as follows. In Section (2) we review the essential ingredients and terminology used throughout the work. We outline the different types of boundary conditions relevant for our analysis. Section (3) presents the general strategy for computing symmetry-resolved entanglement entropy (SREE) by decomposing the entanglement into contributions from individual representations. We examine how different choices of boundary states inserted at the entangling surface of a bipartite system influence the resolution of entanglement. In this context, motivated by the SymTFT construction of [1], we provide a general formula for SREE that applies to a broad class of theories, including non-unitary and non-diagonal RCFTs, and accommodates various admissible boundary conditions. In Section (4) we compute SREE in several unitary models and verify the consistency of the corresponding boundary entropies using the generalized Affleck–Ludwig boundary entropy formula. We also attempt to resolve the symmetry sectors of the non-diagonal  $SU(2)_{10}$  WZW model with  $E_6$  type classification, and discuss the limitations of BCFT techniques in resolving its  $\frac{1}{2}E_6$  categorical symmetry. Nevertheless, we demonstrate that such limitations are not universal: for example, we explicitly resolve the  $\mathbb{Z}_3$  symmetry (an invertible symmetry) in the three-state Potts model, which stands as a non-diagonal RCFT that admits consistent symmetry resolution using BCFT techniques. Finally, in Section (5) we turn to several non-unitary models and show that the modified Affleck–Ludwig formula continues to hold in these cases as well, thereby extending our analysis beyond the domain of unitary RCFTs. We conclude with a discussion in Section (6).

## 2 Background and basic setup

We begin by reviewing the fundamental principles and structural properties of RCFTs. An RCFT is distinguished by the existence of only finitely many primary fields together with a rational central charge  $c$ . A central role in their formulation is played by the construction of the Vertex Operator Algebra (VOA), which provides the algebraic foundation for the theory. In general, the partition function of an RCFT takes the form [115],

$$Z(\tau, \bar{\tau}) = \sum_{i,j} M_{ij} \chi_i(\tau) \bar{\chi}_j(\bar{\tau}) \quad i, j \in \text{Primary spectrum} \quad (2.1)$$

where, the characters  $\chi_i(\tau)$  are defined as,

$$\chi_i(\tau) = \text{Tr}_{\mathcal{H}_{R_i}} q^{L_0 - \frac{c}{24}} \bar{q}^{\bar{L}_0 - \frac{c}{24}}, \text{ with, } q = e^{2\pi i \tau} \quad (2.2)$$

along with the Hamiltonian,

$$H = L_0 + \bar{L}_0. \quad (2.3)$$

Now the degeneracy matrix  $M_{ij}$  in (2.1) need not be diagonal always. When  $M_{ij} = \delta_{ij}$ , we call the RCFT a diagonal one; otherwise, we call it a non-diagonal RCFT. In the next subsection, we will briefly introduce the notion of boundaries and defects, which will be relevant for our computation of SREE in the subsequent sections.

### Introducing defects and conformal boundary conditions in RCFT

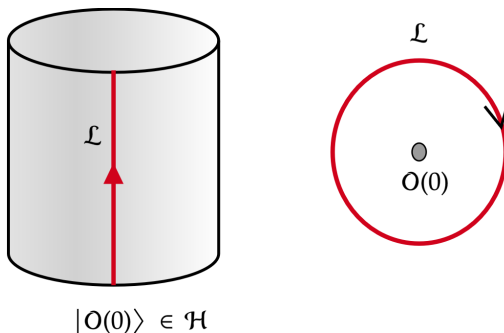


**Figure 1:** Inserting a topological defect line( $\mathcal{L}$ ) along the Euclidean time direction (left), which, after the conformal transformation (from cylinder to plane), acts on the local operator (right).

A conformal defect can be understood as an extended operator that extends along the Euclidean time direction while remaining localized in the spatial dimensions [17, 19] as shown in Fig. (1). For non-invertible defects, the corresponding defect lines are known to be equivalent to the charge operators in the associated invertible theory. This correspondence offers a conceptual framework for computing the SREE through the evaluation of charge moments [53, 54, 116]. In contrast, our work adopts a different strategy: we employ the established BCFT formalism to determine the SREE [72]. Regardless of the chosen approach, the SREE can ultimately be expressed in terms of the quantum dimensions of the defect lines contributing to each symmetry sector. For the construction of the boundary states, we choose the conformal Cardy states. These cardy states are the linear combination of the Ishibashi states with specific coefficients. Ishibashi states are solutions of the Ishibashi condition given by the construction of BCFT as [117–122]<sup>6</sup>,

$$(T(z) - \bar{T}(\bar{z}))|_{\text{bdy}} = 0. \quad (2.4)$$

Now using Virasoro mode decomposition,  $T(z) = \sum_{n=0}^{\infty} \frac{L_n}{z^{n+2}}$  for the Ishibashi condition, we get the following equation,

$$(L_n - L_{-n})|\alpha\rangle = 0 \quad (2.5)$$

<sup>6</sup>For more details, we suggest the reader the following review [123] and the book [124].

where,  $\{L_n\}$  are the Virasoro generators.

**Strong and Weakly symmetric boundary:** We define a boundary weakly symmetric if the symmetry defects can end topologically on it, leading to conserved operators for the Hamiltonian on a strip (open string channel). Similarly, for a boundary becoming strongly symmetric, the relevant boundary state is an eigenstate of the symmetry operators (closed string channel). These two notions are degenerate for invertible symmetries but quite different for non-invertible symmetries. We define them as follows. The boundary is called *strongly symmetric* if for every defect line  $\mathcal{L}_a$  for  $a \in \mathcal{C}$  there a boundary state  $\|B\rangle\rangle$  which satisfies the following [87, 93],

$$\mathcal{L}_a\|B\rangle\rangle = \langle\mathcal{L}_a\rangle\|B\rangle\rangle \quad \forall a \in \mathcal{C} \quad (2.6)$$

and similarly a boundary is called *weakly symmetric* if the following equation holds,

$$\mathcal{L}_a\|B\rangle\rangle = \|B\rangle\rangle + \dots \quad \forall a \in \mathcal{C} \quad (2.7)$$

where the ellipsis denotes the sum of other Cardy boundary states present in the theory. If there is a defect line with a non-integer quantum dimension, it turns out that one can not find any strongly symmetric boundary state [84, 87].

**Cloaking boundary.** Apart from the standard Cardy boundary conditions, we also consider a special class of boundary states known as *cloaking boundary states* [94, 95, 125, 126]. These boundary conditions play a central role in symmetry resolution because they are constructed to be invisible to a chosen set of topological defect lines. Let  $\mathcal{J} \subset \mathcal{C}$  denote a closed sub-fusion category generated by a set of simple objects (which may include both invertible and non-invertible defect lines). We also define  $\mathcal{I} \subset \text{Irr}(\mathcal{C})$  as the collection of all simple objects whose Ishibashi states survive the projection onto the  $\mathcal{J}$ -subsector; equivalently,  $\mathcal{I}$  consists of all labels appearing in the fusion closure of  $\mathcal{J}$ .

A boundary condition is said to be *cloaked* with respect to  $\mathcal{J}$  if its Ishibashi components are invisible to the fusion action of every line in  $\mathcal{J}$ , i.e., the defect line passes through the boundary, unlike the Cardy states, where the lines end. This invisibility condition is imposed by requiring that the row of the modular  $S$ -matrix indexed by  $x$  agrees with the vacuum row when restricted to the columns labeled by  $\mathcal{J}$ . Explicitly, the allowed Ishibashi labels  $x \in \mathcal{I}$  satisfy

$$\left\{ x \in \mathcal{I}, \quad \frac{S_{xj}}{S_{x1}} = \frac{S_{1j}}{S_{11}} \quad \forall j \in \mathcal{J} \right\}. \quad (2.8)$$

Here  $S_{ij}$  denotes the elements of the modular  $S$ -matrix. Whenever the above condition holds, the Ishibashi state  $|x\rangle\rangle$  contributes to the cloaking boundary. The properly normalized

cloaking boundary state is <sup>7</sup>

$$|\gamma(\delta)\rangle\rangle = \delta_0 \text{Dim}(\mathcal{J}) \sum_{x \in \mathcal{I}} \sqrt{S_{x1}} |x\rangle\rangle, \quad (2.8)$$

where the total quantum dimension of the sub-fusion category  $\mathcal{J}$  is defined by

$$\text{Dim}(\mathcal{J}) = \sqrt{\sum_{a \in \mathcal{J}} d_a^2}.$$

In the following section, we explain how cloaking boundary states are incorporated into the computation of symmetry-resolved entanglement entropy and discuss the role played by different choices of  $\mathcal{J}$ .

### 3 Symmetry resolved entanglement entropy (SREE)

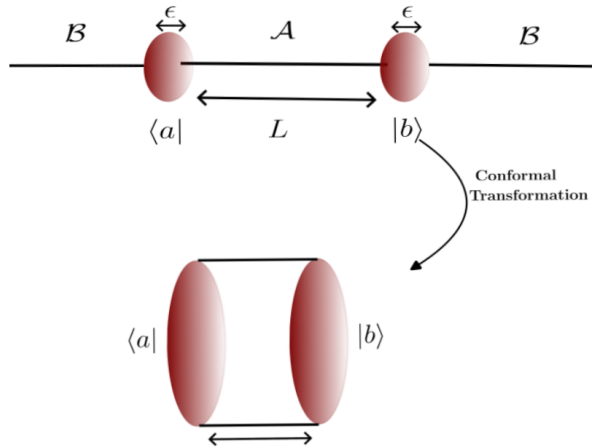


**Figure 2:** For a set of intervals A and B, as the Hilbert space is not a direct product, we have put conformal boundary conditions with two small  $\epsilon$  circles at the entangling surface, which turn into two different Cardy boundary states after conformal mapping to an annulus.

We consider a  $(1+1)$  dimensional quantum system endowed with an internal symmetry and partition it into two complementary subsystems,  $A$  and  $B$ . In order to compute the entanglement entropy of subsystem  $A$  of length  $L$  with  $B$ , we have traced out the subsystem  $B$ , and this configuration is conformally equivalent to an annulus of width  $W = 2 \log\left(\frac{L}{\epsilon}\right)$ , see Fig. (2). Let  $\mathcal{Q}$  denote the conserved charge operator generating the symmetry. We assume that the total charge decomposes additively as

$$\mathcal{Q} = \mathcal{Q}_A \oplus \mathcal{Q}_B. \quad (3.1)$$

---

<sup>7</sup> $\delta_0$  is a normalization constant which can be appropriately chosen following [94, 95, 125].

If the global state of the system is an eigenstate of  $\mathcal{Q}$ , it follows that

$$[\rho, \mathcal{Q}] = 0, \quad (3.2)$$

where  $\rho$  is the density matrix of the full system. By tracing over the degrees of freedom of  $B$ , we obtain the reduced density matrix  $\rho_A = \text{Tr}_B \rho$ , which commutes with the subsystem charge operator  $\mathcal{Q}_A$ . Consequently,  $\rho_A$  has a block-diagonal structure (where each block is denoted by  $\mathcal{R}_\rho$ ), with each block labeled by an eigenvalue  $q_\rho$  of  $\mathcal{Q}_A$ :

$$\rho_A = \bigoplus_i \rho_A(q_\rho). \quad (3.3)$$

Each block  $\rho_A(q_\rho)$  is obtained by projecting  $\rho_A$  onto the eigenspace of  $\mathcal{Q}_A$  with corresponding eigenvalue. Through this decomposition, one can define symmetry-resolved entanglement measures. Following [53, 54, 69, 127], the symmetry-resolved Rényi entropy, which quantifies the entanglement between subsystems  $A$  and  $B$  within a fixed charge sector  $\mathcal{R}_\rho$ , is defined as

$$S_n(\mathcal{R}_\rho) := \frac{1}{1-n} \log \text{Tr} \rho_A(q_\rho)^n = \frac{1}{1-n} \log \left( \frac{Z(q^n, \mathcal{R}_\rho)}{Z^n(q, \mathcal{R}_\rho)} \right). \quad (3.4)$$

Here,  $Z(q)$  denotes the full annulus partition function in the open-string channel and closed-string channel related by modular  $S$  transformation [122, 128], expressed as <sup>8</sup>,

$$Z_{B_1|B_2}(q) = \sum_{i \in \rho \in \text{Irr}(\mathcal{C})} \bar{\mathcal{N}}_{iB_1}^{B_2} \chi_i(q) \stackrel{!}{=} \langle\langle B_1 | \tilde{q}^{L_0 - \frac{c}{24}} | B_2 \rangle\rangle \quad (3.5)$$

where  $B_1$  and  $B_2$  label the boundary Cardy states and  $q = e^{-\frac{2\pi^2}{W}}$ ,  $\tilde{q} = e^{-2W}$ . Throughout this work, we adopt the notation  $Z(q)$  in place of  $Z_{a|b}(q)$ . In subsequent sections, the structure and interpretation of the coefficients  $n_{ia}^b$  will be elaborated in detail. Accordingly,  $Z(q, \mathcal{R}_\rho)$  refers to the sector of the full partition function corresponding to the symmetry representation denoted by  $\mathcal{R}_\rho$ . For 1 + 1D RCFT, the global symmetry is generated by topological defect lines (TDLs), and they form a fusion category. In order to resolve the entanglement Rényi entropy with respect to the fusion category of the underlying TDLs, the partition functions of each irreducible sectors can be extracted from the full annulus partition function by looking at the action of the TDLs on the primary fields rather than computing charged moments [69]<sup>9</sup>.

---

<sup>8</sup>In light of [95], and as we will also observe in later computations, the open-closed duality is anomalous: the correspondence does not hold exactly for the cloaking boundary state. This anomaly appears in the open-string spectrum, where some coefficients become non-integer. Nevertheless, in our analysis we continue to use this duality, and the final result still admits a consistent probabilistic interpretation. Strictly speaking, the anomaly may introduce an additional correction to the SREE, but this can be absorbed into the universal term. We thank Brandon Rayhaun for emphasizing this point.

<sup>9</sup>For the computation of charged moments, we have to compute the projectors in terms of the  $F$ -symbols. For generic RCFT, it is very hard to compute these symbols. For more detail about the  $F$ -symbols upto rank 7, see [129, 130].

## Boundary conditions and SREE

In this section, we briefly review some subtleties in the choice of boundary states and their consequences for the symmetry-resolved Rényi entropies (SRRE). For illustration, suppose there are  $N$  irreducible blocks; the Rényi entropy for the  $\rho$ 'th block admits the following asymptotic behaviour in the high energy limit  $q \rightarrow 1$  or  $\tilde{q} \rightarrow 0$ ,

$$S_n(\mathcal{R}_\rho) = \frac{1}{1-n} \log \left( \frac{Z(q^n, \mathcal{R}_\rho)}{Z^n(q, \mathcal{R}_\rho)} \right), \quad \frac{Z(q^n, \mathcal{R}_\rho)}{Z^n(q, \mathcal{R}_\rho)} \xrightarrow{\tilde{q} \rightarrow 0} p_\rho^{n-1} \tilde{q}^{\left(n-\frac{1}{n}\right) \frac{c_{\text{eff}}}{24}}, \quad (3.6)$$

with

$$Z(q^n, \mathcal{R}_\rho) \stackrel{\tilde{q} \rightarrow 0}{\sim} p_\rho \chi_{\text{GS}}(\tilde{q}^{1/n}) \quad (3.7)$$

where  $c_{\text{eff}} = c - 24\Delta_{\text{GS}}$  and  $\Delta_{\text{GS}}$  is the conformal dimension of the ground state (for unitary theory ground state is the vacuum state with  $\Delta_{\text{GS}} = 0$ , but non-zero for non-unitary theory). In this limit, the SREE for the irreducible block becomes

$$S_n(\mathcal{R}_\rho) = \frac{c_{\text{eff}}}{6} \left( \frac{n+1}{n} \right) \log \left( \frac{L}{\epsilon} \right) + \log(p_\rho) + \dots \quad (3.8)$$

From this we can get the symmetry-resolved entanglement entropy (SREE) by taking  $n \rightarrow 1$  limit. Our aim is not only to compute the SREE but also to relate the  $p_\rho$ 's to modular data and topological quantities. We therefore propose the following prescriptions for different classes of boundary states.

### Weakly symmetric boundary condition

For a weakly symmetric boundary state, the SREE in the charge sector labelled by  $\rho \in \text{Irr}(\mathcal{C})$  takes the form

$$S(\mathcal{R}_\rho) = \frac{c_{\text{eff}}}{3} \log \left( \frac{L}{\epsilon} \right) + \log(g_1 g_2) + \log \left( \frac{d_\rho N_{\rho B_1}^{B_2}}{d(B_1 \otimes B_2)} \right), \quad (3.9)$$

where the  $g_i$ 's are boundary entropies and, if a block contains several irreducible elements (this scenario may appear when the full resolution is not possible), a sum over the block index  $\rho$  is implied. For multiplicity-free fusion of the defect lines, one finds

$$d(B_1 \otimes B_2) = \sum_{\rho} d_{\mathcal{L}_\rho}, \quad (3.10)$$

so that (3.9) reduces to

$$S(\mathcal{R}_\rho) = \frac{c_{\text{eff}}}{3} \log \left( \frac{L}{\epsilon} \right) + \log(g_1 g_2) + \log \left( \frac{d_\rho}{\sum_{\rho \in \text{Irr}(\mathcal{C})} d_\rho} \right). \quad (3.11)$$

**Remark.** For a weakly symmetric boundary, one may regard  $\rho$  as an element of  $B_1 \otimes B_2$ . The fusion product  $B_1 \otimes B_2$  then generates the entire subfusion sector. Equation (3.11) holds essentially in multiplicity-free situations, i.e. when there are no fusion multiplicities and each irreducible block carries a single character.

The expression (3.9) can be viewed as a special instance of a more general relation,

$$S(\mathcal{R}_\rho) = \frac{c_{\text{eff}}}{3} \log\left(\frac{L}{\epsilon}\right) + \log(g_1 g_2) + \log\left(\frac{d_\rho \overline{\mathcal{N}}_{\rho B_1}^{B_2}}{d_{B_1} d_{B_2}}\right), \quad (3.12)$$

which applies to a broader class of boundary conditions. Here  $\overline{\mathcal{N}}_{\rho B_1}^{B_2}$  denotes the boundary fusion coefficient defined via the action of a topological defect line on a boundary state<sup>10</sup>:

$$\mathcal{L}_\rho \|B_1\rangle\rangle = \overline{\mathcal{N}}_{\rho B_1}^{B_2} \|B_2\rangle\rangle + \sum \|CS\rangle\rangle. \quad (3.13)$$

Using the state–operator correspondence together with the Cardy construction, one finds the explicit action (for diagonal RCFT) [128],

$$\mathcal{L}_\rho \|B_i\rangle\rangle = \sum_{j=1}^N \frac{S_{ij}}{\sqrt{S_{1j}}} \mathcal{L}_\rho |j\rangle\rangle = \sum_{j=1}^N \frac{S_{ij}}{\sqrt{S_{1j}}} \frac{S_{\rho j}}{S_{1j}} |j\rangle\rangle. \quad (3.14)$$

Note that both the Cardy and Ishibashi states are not primary states. The Ishibashi state can be expanded as a sum over a primary and its descendants:

$$|\mu\rangle\rangle = \sum_{N=0}^{\infty} |\mu, N\rangle \otimes |\bar{\mu}, N\rangle, \quad (3.15)$$

where  $\{|\mu, N\rangle\}$  is an orthonormal basis of the irreducible module  $\mathcal{H}_\mu$ . The primary state is  $|\mu, 0\rangle$ , and the Virasoro descendants are generated as

$$|\mu, N\rangle = L_{-n_1} L_{-n_2} \cdots L_{-n_k} |\mu, 0\rangle, \quad n_1 + n_2 + \cdots + n_k = N. \quad (3.16)$$

Consider now the action of  $\mathcal{L}_\rho$  on the Ishibashi state:

$$\begin{aligned} \mathcal{L}_\rho |\mu\rangle\rangle &= \sum_{N=0}^{\infty} \mathcal{L}_\rho |\mu, N\rangle \otimes |\bar{\mu}, N\rangle = \sum_{N=0}^{\infty} \mathcal{L}_\rho L_{-n_1} L_{-n_2} \cdots L_{-n_k} |\mu, 0\rangle \otimes |\bar{\mu}, N\rangle, \\ &= \sum_{N=0}^{\infty} L_{-n_1} L_{-n_2} \cdots L_{-n_k} \mathcal{L}_\rho |\mu, 0\rangle \otimes |\bar{\mu}, N\rangle, \\ &\stackrel{\text{state-operator}}{=} \sum_{N=0}^{\infty} L_{-n_1} L_{-n_2} \cdots L_{-n_k} \underbrace{\mathcal{L}_\rho \Phi_\mu}_{S_{\rho\mu}/S_{1\mu}} |0\rangle \otimes |\bar{\mu}, N\rangle \longrightarrow \frac{S_{\rho\mu}}{S_{1\mu}} |\mu\rangle\rangle. \end{aligned} \quad (3.17)$$

<sup>10</sup>We propose this interpretation of the working formula without invoking the SymTFT construction, relying instead on a purely 2d RCFT analysis, in contrast to [1].

Since  $\mathcal{L}_\rho$  is a symmetry generator, it commutes with all Virasoro generators. Thus, even though Ishibashi states are not primary, the action of  $\mathcal{L}_\rho$  on those states mimics that of primary fields, unlike Cardy states. From (3.14), one can then recombine terms to identify the coefficients  $\overline{\mathcal{N}}_{\rho B_1}^{B_2}$ . Open–closed duality further imposes the consistency condition

$$d_{B_1} d_{B_2} = \sum_{\rho \in \text{Irr}(\mathcal{C})} \overline{\mathcal{N}}_{\rho B_1}^{B_2} d_\rho. \quad (3.18)$$

### Verification of (3.18) for real, symmetric modular data

The annulus partition function in the open-string channel is

$$Z_{B_1|B_2}(q) = \sum_\rho \overline{\mathcal{N}}_{\rho B_1}^{B_2} \chi_\rho(q) = \sum_{\rho, i} \overline{\mathcal{N}}_{\rho B_1}^{B_2} S_{\rho i} \chi_i(\tilde{q}), \quad \tilde{q} \xrightarrow{\sim} \sum_\rho \overline{\mathcal{N}}_{\rho B_1}^{B_2} S_{\rho 1} \chi_1(\tilde{q}) + \dots \quad (3.19)$$

In the closed channel, the corresponding partition function reads

$$Z_{B_1|B_2}(\tilde{q}) = \langle\langle B_1 \| \tilde{q}^{L_0 - \frac{c}{24}} \| B_2 \rangle\rangle = \sum_{i, j} \frac{S_{B_2 i}}{\sqrt{S_{1i}}} \frac{S_{B_1 j}}{\sqrt{S_{1j}}} \delta_{ij} \chi_j(\tilde{q}) \quad (3.20)$$

$$\tilde{q} \xrightarrow{\sim} \frac{S_{B_2 1} S_{B_1 1}}{S_{11}} \chi_1(\tilde{q}) + \dots$$

Matching the leading terms from both channels yields

$$\frac{1}{S_{11}} \sum_\rho \overline{\mathcal{N}}_{\rho B_1}^{B_2} S_{\rho 1} = d_{B_1} d_{B_2} \quad \implies \quad d_{B_1} d_{B_2} = \sum_\rho \overline{\mathcal{N}}_{\rho B_1}^{B_2} d_\rho, \quad (3.21)$$

as claimed in (3.18). A similar derivation holds for more general modular data with complex entries.

### Why (3.9) holds for weakly symmetric boundaries

For weakly symmetric Cardy boundaries, the action of topological defect lines on boundary Ishibashi states closes according to the bulk fusion algebra [131]<sup>11</sup>:

$$\mathcal{L}_\rho \|\Phi_i\rangle\rangle = \sum_{j=1}^N N_{\rho i}^j \|\Phi_j\rangle\rangle, \quad (3.22)$$

where the bulk fusion coefficients are given by

$$\Phi_\rho \times \Phi_i = \sum_{j=1}^N N_{\rho i}^j \Phi_j, \quad N_{\rho i}^j = \sum_{n=1}^N \frac{S_{\rho n} S_{in} S_{nj}^*}{S_{1n}}. \quad (3.23)$$

Although there is no strict one-to-one correspondence between Cardy boundary states and bulk primaries, the structural similarity between (3.22) and (3.23) justifies identifying the defect action with the associated fusion data. This correspondence explains the validity of the simpler formula (3.9) in the weakly symmetric case.

<sup>11</sup>Interested readers are referred to [132] for some applications of these boundary conditions in the context of Ising model for describing edge modes.

### Strongly (and possibly cloaking) boundary condition

The prescription (3.11) fails in the presence of strongly symmetric boundary states. For a strongly symmetric boundary state, the topological defect line acts simply by its quantum dimension:

$$\mathcal{L}_\rho \|B\rangle\rangle = d_\rho \|B\rangle\rangle \implies \overline{\mathcal{N}}_{\rho B}^B = d_\rho. \quad (3.24)$$

Substituting this relation into (3.12) and using the open-closed identity (3.18) yields the SREE <sup>12</sup>

$$S(\mathcal{R}_\rho) = \frac{c_{\text{eff}}}{3} \log\left(\frac{L}{\epsilon}\right) + \log(g_1 g_2) + \log\left(\frac{d_\rho^2}{\sum_{\rho \in \text{Irr}(\mathcal{C})} d_\rho^2}\right). \quad (3.25)$$

The formula (3.25) is expected to apply also to the cloaking boundary state [94, 95] introduced in (2.8). In many diagonal RCFTs, the cloaking state coincides with the identity Ishibashi state  $|\mathbb{I}\rangle\rangle$  [94, 95], for which the defect acts by its quantum dimension:

$$\mathcal{L}_\rho |\mathbb{I}\rangle\rangle = d_\rho |\mathbb{I}\rangle\rangle, \quad (3.26)$$

so that  $\overline{\mathcal{N}}_{\rho \mathbb{I}}^{\mathbb{I}} = d_\rho$  and Eq. (3.25) follows directly. We stress, however, that although (3.25) holds in these (cloaking) examples, the derivations (e.g (3.21)) employed for the Cardy boundary states do not carry over in a straightforward way to cloaking boundaries (as cloaking states are not physical Cardy states).

## 4 Computing SREE in Unitary Rational CFT

In this section, we investigate symmetry resolution in both unitary diagonal and non-diagonal RCFTs. For diagonal models, we primarily focus on the Tambara-Yamagami (TY) symmetry resolution in the Ising and tetracritical Ising CFTs. For non-diagonal RCFTs, we examine two representative cases: the  $E_6$  theory and its  $\frac{1}{2}E_6$  fusion ring, and the  $\mathbb{Z}_3$  symmetry resolution in the three-state Potts model.

### 4.1 Symmetry resolution with respect to Tambara-Yamagami (TY) Fusion Category for Ising CFT

The simplest unitary Virasoro minimal model, namely the critical Ising model, is the prototype example for two-dimensional rational CFT. It has three primaries,  $\{\mathbb{I}, \varepsilon, \sigma\}$ , and their non-trivial fusions are

$$\varepsilon \times \varepsilon = \mathbb{I}, \quad \varepsilon \times \sigma = \sigma, \quad \sigma \times \sigma = \mathbb{I} + \varepsilon. \quad (4.1)$$

This is a diagonal rational CFT. So, it has three topological defects labeled by the primaries, namely,  $\{\mathcal{L}_{\mathbb{I}}, \mathcal{L}_\varepsilon, \mathcal{L}_\sigma\} = \mathcal{C}$  and their action on the primaries is summarized in Table (1).

<sup>12</sup>For cloaking states the formula in (3.25) matches with [1, 81].

Defect line	$\mathbb{I}$	$\varepsilon$	$\sigma$
$\mathcal{L}_{\mathbb{I}}$	1	1	1
$\mathcal{L}_{\varepsilon}$	1	1	-1
$\mathcal{L}_{\sigma}$	$\sqrt{2}$	$-\sqrt{2}$	0

**Table 1:** Action of the TY category on the primaries .

We want to study symmetry-resolved entanglement entropy for this TY fusion category symmetry. In order to do that, we need a strongly symmetric or weakly symmetric entangled boundary condition according to [1, 83, 84, 87]. But it turns out that for this case, there is no such boundary at the entangled surfaces. However, one can use the cloaking boundary condition [94, 95] for the purpose of symmetry resolution. For the critical Ising model, it turns out that the Ishibashi state gives the cloaking boundary state that corresponds to the identity primary [95]

$$\|\gamma(\delta)\rangle\rangle = |\mathbb{I}\rangle\rangle. \quad (4.2)$$

Now, we can compute the annulus partition function in the closed string channel when we sandwich the cloaking state (4.2) at the boundary.

$$\begin{aligned} Z(\tilde{q}) &= \langle\langle \gamma(\delta) \| \tilde{q}^{L_0 - \frac{c}{24}} \| \gamma(\delta) \rangle\rangle, \\ &= \chi_1(\tilde{q}) \quad \text{in closed string channel,} \\ &\stackrel{!}{=} \frac{1}{2}\chi_1(q) + \frac{1}{2}\chi_2(q) + \frac{1}{\sqrt{2}}\chi_3(q) \quad \text{in open string channel.} \end{aligned}$$

The TY fusion category has three elements, and there are three representations (each irreducible block is represented by  $\mathcal{R}_\rho$ ,  $\rho = 1, 2, 3$ ). Hence, following the discussion presented in Sec. (3), the reduced density matrix can be decomposed into three blocks. From the Table (1), we can see the action of  $\mathcal{C}$  on each primary is different; therefore, we can write the symmetry-resolved partition functions as,

$$Z(q^n, \mathcal{R}_1) = \frac{\frac{1}{2}\chi_1(q^n)}{Z^n(q)}, \quad Z(q^n, \mathcal{R}_2) = \frac{\frac{1}{2}\chi_2(q^n)}{Z^n(q)}, \quad Z(q^n, \mathcal{R}_3) = \frac{\frac{1}{\sqrt{2}}\chi_3(q^n)}{Z^n(q)}. \quad (4.3)$$

Now, using (3.4), we can compute the symmetry-resolved  $n$ th Rényi . As discussed in (3.6), in the high-energy limit, the leading contribution comes from the vacuum. Therefore,

$$\frac{Z(q^n, \mathcal{R}_1)}{Z^n(q, \mathcal{R}_1)} \stackrel{\tilde{q} \rightarrow 0}{\sim} \left(\frac{1}{4}\right)^{1-n} \tilde{q}^{(n-\frac{1}{n})\frac{c}{24}} \quad (4.4)$$

and SREE for this block becomes

$$S(\mathcal{R}_1) = \frac{c}{6} \left(\frac{n+1}{n}\right) \log\left(\frac{L}{\epsilon}\right) + \log\frac{1}{4} + \dots \quad (4.5)$$

where the constant term

$$\log \frac{1}{4} = \log \left( \frac{d_{\mathcal{R}_1}^2}{\sum_{\mathcal{R}_i} d_{\mathcal{R}_i}^2} \right) + \log(\langle\langle \gamma(\delta) \| \Omega \rangle \langle \Omega | \gamma(\delta) \rangle\rangle). \quad (4.6)$$

where,  $d_{\mathcal{R}_1} = 1$ ,  $\sum_{\mathcal{R}_i} d_{\mathcal{R}_i}^2 = 4$ , and  $\log(\langle\langle \gamma(\delta) \| \Omega \rangle \langle \Omega | \gamma(\delta) \rangle\rangle) = 0$  corresponds to the Affleck-Ludwig boundary entropy [133]. Similar result can be obtained for  $S(\mathcal{R}_2)$ , and

$$S(\mathcal{R}_3) = \frac{c}{6} \left( \frac{n+1}{n} \right) \log \left( \frac{L}{\epsilon} \right) + \log \frac{1}{2} + \dots, \quad (4.7)$$

where the constant term

$$\log \frac{1}{2} = \log \left( \frac{d_{\mathcal{R}_3}^2}{\sum_{\mathcal{R}_i} d_{\mathcal{R}_i}^2} \right) + \log(\langle\langle \gamma(\delta) \| \Omega \rangle \langle \Omega | \gamma(\delta) \rangle\rangle). \quad (4.8)$$

Here  $d_{\mathcal{R}_3} = \sqrt{2}$  is the quantum dimension of  $\mathcal{L}_\sigma$ . We observe that equation (3.25) is satisfied in this example when using the specified boundary states, known as the cloaking states. Through a detailed examination of this explicit case, it becomes clear that symmetry resolution in the Ising CFT with respect to the TY fusion ring cannot be achieved using the standard procedure, as no weakly symmetric state exists in this case. However, by employing the cloaking state, we demonstrate that such a resolution becomes feasible. To the best of our knowledge, this work presents the first TY-resolution of the Ising CFT in the literature.

## 4.2 Symmetry resolution for $\mathcal{M}(6, 5)$

We now analyze the symmetry resolution of the diagonal  $\mathcal{M}(6, 5)$  theory. Interestingly, in this case, there are two natural choices of sub-fusion categories, which we treat separately. For the larger sub-fusion category we find that no weakly symmetric boundary state exists, but we can still perform the resolution using an appropriate cloaking boundary state. In contrast, for the smaller sub-fusion category, a weakly symmetric boundary state is available, and the symmetry resolution proceeds accordingly.

**Tetracritical Ising model.** The diagonal minimal model corresponding to the modular data of  $\mathcal{M}(6, 5)$ , the tetracritical Ising model [6, 87], is another example of a diagonal RCFT. The model  $\mathcal{M}(6, 5)$  has central charge  $c = \frac{4}{5}$  and admits ten simple Verlinde lines, which we label as <sup>13</sup>

$$I, C = \mathcal{L}_Y, M = \mathcal{L}_Z, W = \mathcal{L}_X, MW, CW, N, CN, WN, CWN. \quad (4.9)$$

---

<sup>13</sup>In contrast, for the Potts CFT, one of the simple TDLs is  $N$ , satisfying  $N \times N = 1 + \eta + \bar{\eta}$ , which is a  $\mathbb{Z}_3$ -TY line. In the diagonal theory, however, we instead encounter the composite line  $M = \eta + \bar{\eta}$  with  $N \times N = I + M$ , which is not strictly of TY type.

Among these lines the subset  $\{\mathcal{L}_{\mathbb{I}}, C, N, CN, M\}$  closes into a TY-type sub-fusion with the nontrivial fusion rules

$$C^2 = I, \quad M^2 = I + M + C, \quad N^2 = I + M. \quad (4.10)$$

We study symmetry resolution with respect to these five simple TDLs. The full fusion category contains ten bulk primaries,

$$\mathbb{I}, Y, \varepsilon, X, Z, \sigma, \Phi_{4,4}, \Phi_{2,2}, \Phi_{4,2}, \Phi_{3,2}. \quad (4.11)$$

To identify the irreducible charge blocks, one first determines the action of the TDLs on these primaries; this action is displayed in the Table (2).

Defect line	$\mathbb{I}$	$Y$	$\varepsilon$	$X$	$Z$	$\sigma$	$\Phi_{4,4}$	$\Phi_{2,2}$	$\Phi_{4,2}$	$\Phi_{3,2}$
$I$	1	1	1	1	1	1	1	1	1	1
$M$	2	2	2	2	-1	-1	0	0	0	0
$C$	1	1	1	1	1	1	-1	-1	-1	-1
$N$	$\sqrt{3}$	$-\sqrt{3}$	$-\sqrt{3}$	$\sqrt{3}$	0	0	-1	-1	1	1
$CN$	$\sqrt{3}$	$-\sqrt{3}$	$-\sqrt{3}$	$\sqrt{3}$	0	0	1	1	-1	-1

**Table 2:** Action of the TDLs on the  $\mathcal{M}(6,5)$  primaries of the tetracritical Ising model.

From Table (2), one sees that there are five irreducible blocks, each containing two primaries. In the absence of symmetric (weakly symmetric) boundary states, we choose the cloaking boundary, which we take to be the identity Ishibashi state,  $|\langle\gamma(\delta)\rangle\rangle = |\langle\mathbb{I}\rangle\rangle$ . The annulus partition function in the closed-string channel is

$$\begin{aligned}
Z(\tilde{q}) &= \langle\langle\gamma(\delta)|\tilde{q}^{L_0 - \frac{c}{24}}|\gamma(\delta)\rangle\rangle = \chi_1(\tilde{q}), \\
&\stackrel{!}{=} \sqrt{\frac{1}{15}\left(\frac{5}{8} - \frac{\sqrt{5}}{8}\right)}\chi_{\mathbb{I}}(q) + \sqrt{\frac{1}{15}\left(\frac{5}{8} - \frac{\sqrt{5}}{8}\right)}\chi_Y(q) + \sqrt{\frac{1}{15}\left(\frac{\sqrt{5}}{8} + \frac{5}{8}\right)}\chi_{\varepsilon}(q) \\
&\quad + \sqrt{\frac{1}{15}\left(\frac{\sqrt{5}}{8} + \frac{5}{8}\right)}\chi_X(q) + 2\sqrt{\frac{1}{15}\left(\frac{5}{8} - \frac{\sqrt{5}}{8}\right)}\chi_Z(q) + 2\sqrt{\frac{1}{15}\left(\frac{\sqrt{5}}{8} + \frac{5}{8}\right)}\chi_{\sigma}(q) \\
&\quad + \sqrt{\frac{1}{5}\left(\frac{5}{8} - \frac{\sqrt{5}}{8}\right)}\chi_{4,4}(q) + \sqrt{\frac{1}{5}\left(\frac{5}{8} - \frac{\sqrt{5}}{8}\right)}\chi_{4,2}(q) \\
&\quad + \sqrt{\frac{1}{5}\left(\frac{\sqrt{5}}{8} + \frac{5}{8}\right)}\chi_{2,2}(q) + \sqrt{\frac{1}{5}\left(\frac{\sqrt{5}}{8} + \frac{5}{8}\right)}\chi_{3,2}(q).
\end{aligned} \quad (4.12)$$

The leading contribution to the block partition functions in the  $\tilde{q} \rightarrow 0$  limit is

$$\begin{aligned} Z(q^n, \mathcal{R}_1) &\sim \frac{1}{12} \chi_{\mathbb{I}}(\tilde{q}^{1/n}), & Z(q^n, \mathcal{R}_2) &\sim \frac{1}{12} \chi_{\mathbb{I}}(\tilde{q}^{1/n}), \\ Z(q^n, \mathcal{R}_3) &\sim \frac{1}{3} \chi_{\mathbb{I}}(\tilde{q}^{1/n}), & Z(q^n, \mathcal{R}_4) &\sim \frac{1}{4} \chi_{\mathbb{I}}(\tilde{q}^{1/n}), & Z(q^n, \mathcal{R}_5) &\sim \frac{1}{4} \chi_{\mathbb{I}}(\tilde{q}^{1/n}). \end{aligned} \quad (4.13)$$

Therefore, the symmetry (Cat-)SREE for the  $\rho$ -th irreducible block is

$$S_n(\mathcal{R}_\rho) = \frac{1}{1-n} \log \left( \frac{Z(q^n, \mathcal{R}_\rho)}{Z^n(q, \mathcal{R}_\rho)} \right), \quad \text{with} \quad \frac{Z(q^n, \mathcal{R}_\rho)}{Z^n(q, \mathcal{R}_\rho)} \xrightarrow{\tilde{q} \rightarrow 0} p_\rho^{n-1} \tilde{q}^{(n-\frac{1}{n}) \frac{c_{\text{eff}}}{24}}, \quad (4.14)$$

where the coefficients are  $p_\rho = \frac{1}{12}, \frac{1}{12}, \frac{1}{3}, \frac{1}{4}, \frac{1}{4}$  for the five irreducible blocks, respectively. In the cloaking (identity Ishibashi) boundary choice, this yields the compact form as (3.25),

$$S_n(\mathcal{R}_\rho) = \frac{c_{\text{eff}}}{6} \left( \frac{n+1}{n} \right) \log \left( \frac{L}{\epsilon} \right) + \log(g^2) + \log \left( \frac{d_\rho^2}{\sum_\rho d_\rho^2} \right), \quad \text{with, } g = 1 \quad (4.15)$$

with the quantum dimensions for the five lines given by

$$d_{\mathbb{I}} = 1, \quad d_M = 2, \quad d_C = 1, \quad d_N = \sqrt{3}, \quad d_{CN} = \sqrt{3}.$$

Hence

$$\sum_\rho d_\rho^2 = 1^2 + 2^2 + 1^2 + (\sqrt{3})^2 + (\sqrt{3})^2 = 12, \quad (4.16)$$

which reproduces the numerical prefactors  $p_\rho = \frac{1}{12}, \frac{1}{12}, \frac{1}{3}, \frac{1}{4}, \frac{1}{4}$  quoted above for the five irreducible blocks.

### Resolution with weakly symmetric boundary state:

As observed above, symmetric boundary states do not exist within the sub-fusion sector under consideration. However, one can identify a *weakly symmetric* boundary state by resolving the minimal model  $\mathcal{M}(6, 5)$  with respect to the smaller subset of Verlinde lines  $\{I, C, M\}$ . From the fusion algebra restricted to this subset, it is immediate that the boundary state  $\|M\rangle\rangle$  satisfies the weak symmetry condition. Consequently, the annulus partition function becomes

$$Z(\tilde{q}) = \langle\langle M \| \tilde{q}^{L_0 - \frac{c}{24}} \| M \rangle\rangle = \chi_1(q) + \chi_Y(q) + \chi_Z(q). \quad (4.17)$$

The action of the topological defect lines shows that there are three irreducible blocks. Their annulus block partition functions in the  $\tilde{q} \rightarrow 0$  limit behave as

$$\begin{aligned} Z(q^n, \mathcal{R}_1) &\sim \frac{1}{2} \sqrt{\frac{1}{30} (5 - \sqrt{5})} \chi_1(\tilde{q}^{1/n}), & Z(q^n, \mathcal{R}_2) &\sim \frac{1}{2} \sqrt{\frac{1}{30} (5 - \sqrt{5})} \chi_1(\tilde{q}^{1/n}), \\ Z(q^n, \mathcal{R}_3) &\sim \sqrt{\frac{1}{30} (5 - \sqrt{5})} \chi_1(\tilde{q}^{1/n}). \end{aligned} \quad (4.18)$$

The boundary entropy for this choice is

$$\log(g^2) = \log |\langle\langle M | \mathbb{I} \rangle\rangle|^2 = \log \sqrt{\frac{2}{15} (5 - \sqrt{5})}. \quad (4.19)$$

With the weakly symmetric boundary  $||M\rangle\rangle$  the Cat-SREE in block  $\rho$  reads

$$S_n(\mathcal{R}_\rho) = \frac{c_{\text{eff}}}{6} \left( \frac{n+1}{n} \right) \log \left( \frac{L}{\epsilon} \right) + \log(g^2) + \log \left( \frac{d_\rho N_{\rho B_1}^{B_2}}{d(B_1 \otimes B_2)} \right), \quad (4.20)$$

where, for the lines under consideration,

$$d_{\mathbb{I}} = 1, \quad d_C = 1, \quad d_M = 2, \quad (4.21)$$

and the relevant fusion coefficients are

$$N_{\mathbb{I}, Z}^Z = 1, \quad N_{Y, Y}^Z = 1, \quad N_{Z, Z}^Z = 1. \quad (4.22)$$

Therefore, the symmetry (Cat-)SREE for the  $\rho$ -th irreducible block is

$$S_n(\mathcal{R}_\rho) = \frac{1}{1-n} \log \left( \frac{Z(q^n, \mathcal{R}_\rho)}{Z^n(q, \mathcal{R}_\rho)} \right), \quad \text{with} \quad \frac{Z(q^n, \mathcal{R}_\rho)}{Z^n(q, \mathcal{R}_\rho)} \xrightarrow{\tilde{q} \rightarrow 0} p_\rho^{n-1} \tilde{q}^{(n-\frac{1}{n}) \frac{c_{\text{eff}}}{24}}, \quad (4.23)$$

where the coefficients are  $p_\rho = \frac{1}{6}, \frac{1}{6}, \frac{1}{3}$  for the five irreducible blocks respectively.

### 4.3 Symmetry resolution in non-diagonal RCFTs

Before turning to non-unitary RCFTs, we take a pause and examine key features of symmetry resolution for non-invertible symmetries in non-diagonal rational conformal field theories. Through an explicit example, we highlight the conceptual and technical challenges that distinguish non-diagonal theories from their diagonal counterparts. In particular, we illustrate how symmetry resolution may fail in non-diagonal RCFTs by studying the non-diagonal  $E_6$  model and its associated  $\frac{1}{2}E_6$  fusion ring. We also give the example of  $\mathbb{Z}_3$  resolution in the three-state Potts model [134] and show that, for this case, the resolution is possible.

#### $E_6$ and its $\frac{1}{2}E_6$ symmetry resolution?

We consider  $SU(2)_{10}$  WZW model of  $E_6$ -type [115]. The torus partition function is given by,

$$Z(\tau) = |\chi_0 + \chi_3|^2 + |\chi_{\frac{3}{2}} + \chi_{\frac{7}{2}}|^2 + |\chi_2 + \chi_5|^2 \quad (4.24)$$

where,  $\chi_j(\tau)$  is spin  $j$   $SU(2)$  affine character. The modular S-matrix for  $SU(2)_{10}$  is a  $11 \times 11$  matrix which can be constructed by the following,

$$S_{jj'} = \sqrt{\frac{2}{k+2}} \sin \left( \frac{(2j+1)(2j'+1)\pi}{k+2} \right), \quad \text{with, } k = 10, \quad \text{and, } j, j' = 0, \frac{1}{2}, \dots, 5. \quad (4.25)$$

The  $\frac{1}{2}E_6$  fusion ring consists of three simple TDLs:  $\mathcal{L}_1 = I$ ,  $\mathcal{L}_5 = X$ ,  $\mathcal{L}_3 = Y$ . The fusion of the TDLs can be derived from the matrix ( $\psi$ ) constructed from the eigenvector of the adjacency matrix of  $E_6$ , which can be derived from the Dynkin diagram.

$$\mathcal{A} \left( \begin{array}{cccccc} & 1 & 2 & 3 & 4 & 5 \\ & \bullet & \bullet & \bullet & \bullet & \bullet \\ & \text{---} & \text{---} & \text{---} & \text{---} & \text{---} \\ & & & \text{---} & & \\ & & & \bullet & & \\ & & & 6 & & \end{array} \right) = \begin{pmatrix} 0 & 1 & 0 & 0 & 0 & 0 \\ 1 & 0 & 1 & 0 & 0 & 0 \\ 0 & 1 & 0 & 1 & 0 & 1 \\ 0 & 0 & 1 & 0 & 1 & 0 \\ 0 & 0 & 0 & 1 & 0 & 0 \\ 0 & 0 & 1 & 0 & 0 & 0 \end{pmatrix} \quad (4.26)$$

The  $\psi$ -matrix is given by<sup>14</sup>,

$$\psi_a^j = \begin{pmatrix} a & \frac{1}{2} & b & b & \frac{1}{2} & a \\ b & \frac{1}{2} & a & -a & -\frac{1}{2} & -b \\ c & 0 & -d & -d & 0 & c \\ b & -\frac{1}{2} & a & -a & \frac{1}{2} & -b \\ a & -\frac{1}{2} & b & b & -\frac{1}{2} & a \\ d & 0 & -c & c & 0 & -d \end{pmatrix} \quad (4.27)$$

where,  $a = \frac{1}{2}\sqrt{\frac{1}{6}(3 - \sqrt{3})}$ ,  $b = \frac{1}{2}\sqrt{\frac{1}{6}(\sqrt{3} + 3)}$ ,  $c = \frac{1}{2}\sqrt{\frac{1}{3}(\sqrt{3} + 3)}$ ,  $d = \frac{1}{2}\sqrt{\frac{1}{3}(3 - \sqrt{3})}$ . Here,  $a$  runs over the nodes of the corresponding Dynkin diagram and  $j$  runs over the exponents. The fusion can be computed from the modified Verlinde formula [115, 128, 135, 136],

$$\hat{\mathcal{N}}_{ab}^c := \sum_{j \in \text{Exp}(G)} \frac{\psi_a^j \psi_b^j \psi_c^j}{\psi_1^j} \quad (4.28)$$

where,  $\text{Exp}(G)$  denotes the exponents of the Dynkin graph  $G$ .  $\hat{\mathcal{N}}_{ab}^c$  is the graph fusion coefficient, which is the fusion coefficient of TDLs in RCFT with ADE modular invariance. For  $E_6$ ,  $\text{Exp}(G) = \{0, \frac{3}{2}, 2, 3, \frac{7}{2}, 5\}$ . The exponents select the subset of primaries that are preserved in the modular invariant (more precisely, it selects the primaries that are present in the diagonal block of the multiplicity matrix), these label the Ishibashi states. Now the fusion of  $\frac{1}{2}E_6$  TDLs are given by [6, 137],

$$X^2 = I, \quad Y^2 = I + X + 2Y, \quad XY = YX = Y. \quad (4.29)$$

As we see, the Cardy boundary  $\|Y\rangle\rangle$  is weakly symmetric with respect to the subfusion  $\{I, X, Y\}$ . Now the closed string partition function with this choice of boundary is given

<sup>14</sup>The  $a$  index in the subscript of  $\psi$  should not be confused with the element  $a$  of the matrix.

by<sup>15</sup>,

$$\begin{aligned}
Z_{\text{closed}}(\tilde{q}) &= \langle\langle Y \| \tilde{q}^{L_0 - \frac{c}{24}} \| Y \rangle\rangle, \\
&= \sum_{j \in \text{Exp}(G)} \frac{(\psi_3^j)^2}{S_{1j}} \chi_j(\tilde{q}) = \sum_{\substack{j \in \text{Exp}(G) \\ i \in \mathcal{I}}} \frac{(\psi_3^j)^2}{S_{1j}} S_{ji} \chi_i(q) := \sum_{i \in \mathcal{I}} n_{ia}^a \chi_i(q), \\
&= \chi_0(q) + 2\chi_1(q) + 3\chi_2(q) + 3\chi_3(q) + 2\chi_4(q) + \chi_5(q) = Z_{\text{open}}(q)
\end{aligned} \tag{4.30}$$

where,  $n_{ia}^b = \sum_{j \in \text{Exp}(G)} \frac{\psi_a^j \psi_b^j S_{ij}}{S_{1j}}$ . From (4.30) we observe that the open-string spectrum generated by the boundary  $\|Y\rangle\rangle$  contains  $SU(2)_{10}$  primaries which are absent from the  $E_6$ , i.e., the open string spectrum is not solely inside the physical spectrum of the theory. As a result, the  $\frac{1}{2}E_6$  fusion ring does not act by scalars on those extra open-channel primaries. To be precise,  $\mathcal{L}_a \phi_j = \frac{\psi_a^j}{\psi_1^j} \phi_j$ ,  $\mathcal{L}_i \phi_j = \frac{S_{ij}}{S_{1j}} \phi_j$ , with,  $j \in \text{Exp}(G)$ ,  $i \in \mathcal{I}$ . Hence symmetry resolution based solely on the intrinsic  $\frac{1}{2}E_6$  fusion data is not canonical: one may still decompose the open spectrum with respect to the defect algebra, but the decomposition is in general non-diagonal (action on the defects by the TDLs are via matrices rather than by scalar projectors) and requires embedding the problem into the full  $SU(2)_{10}$  theory. To elaborate further,  $\mathcal{L}_a \phi_i = (D_a)_{i,j} \phi_j$  with,  $i \notin \text{Exp}(G)$ , one can not call it a symmetry. Hence, the notion of symmetry resolution is not defined in the usual sense. As an aside, we may still compute the full entanglement entropy, which is given by,

$$S = \frac{c}{3} \log \left( \frac{L}{\epsilon} \right) + \log(g^2) + \dots \tag{4.31}$$

where the boundary entropy is given by,

$$\log(g^2) = \log |\langle\langle I \| Y \rangle\rangle|^2 = \log(2 + \sqrt{3}). \tag{4.32}$$

### Three state Potts and its $\mathbb{Z}_3$ resolution

In three state Potts model, the  $\mathbb{Z}_3$  fusion ring consists of three simple TDLs:  $I, \eta, \eta^2$ . The fusion of these TDLs is given by,

$$\eta \times \eta = \eta^2, \eta \times \eta^2 = 1, \eta^2 \times \eta^2 = \eta. \tag{4.33}$$

As we see, we do not have any weakly symmetric boundary in the fusion ring. However, we can choose a bigger fusion ring that consists of another simple object  $N$ , which has the following fusion [134]:

$$N \times N = 1 + \eta + \eta^2, N \times \eta = N, N \times \bar{\eta} = N. \tag{4.34}$$

---

<sup>15</sup> $\mathcal{I}$  denotes the full mother spectrum, which is, for our case,  $SU(2)_{10}$ .

As we see,  $N$  can be treated as a *strongly symmetric boundary*, and the annulus open string partition function is given by [135, 136, 138],

$$\begin{aligned} Z(\tilde{q}) &= \langle\langle N \| \tilde{q}^{L_0 - \frac{c}{24}} \| N \rangle\rangle, \\ &= Z(q) = \chi_1(q) + \chi_Y(q) + 2\chi_Z(q). \end{aligned} \quad (4.35)$$

As we see, unlike the  $E_6$  case, the open string spectrum is solely in the Potts spectrum. Now, we study symmetry resolution with respect to the three  $(I, \eta, \eta^2)$  invertible simple TDLs. The full fusion category contains eight bulk primaries, From Table (3), we see that there are

	$I$	$Y$	$Z$	$Z^*$
$I$	1	1	1	1
$\eta$	1	1	$\omega$	$\omega^2$
$\eta^2$	1	1	$\omega^2$	$\omega$

**Table 3:** Action of TDLs on the open string spectrum primaries [139, 140].

three irreducible blocks corresponding to the three simple TDLs:  $(I, Y)$ ,  $Z$ ,  $Z^*$ . The leading contributions to the block partition functions in the  $\tilde{q} \rightarrow 0$  limit are

$$\begin{aligned} Z(q^n, \mathcal{R}_1) &\sim \sqrt{\frac{1}{30}(5 - \sqrt{5})} \chi_{\mathbb{I}}(\tilde{q}^{1/n}), & Z(q^n, \mathcal{R}_2) &\sim \sqrt{\frac{1}{30}(5 - \sqrt{5})} \chi_{\mathbb{I}}(\tilde{q}^{1/n}), \\ Z(q^n, \mathcal{R}_3) &\sim \sqrt{\frac{1}{30}(5 - \sqrt{5})} \chi_{\mathbb{I}}(\tilde{q}^{1/n}). \end{aligned} \quad (4.36)$$

Therefore, the symmetry resolved Rényi entropy for the  $\rho$ -th irreducible block is

$$S_n(\mathcal{R}_\rho) = \frac{1}{1-n} \log \left( \frac{Z(q^n, \mathcal{R}_\rho)}{Z^n(q, \mathcal{R}_\rho)} \right), \quad \text{with} \quad \frac{Z(q^n, \mathcal{R}_\rho)}{Z^n(q, \mathcal{R}_\rho)} \xrightarrow{\tilde{q} \rightarrow 0} p_\rho^{n-1} \tilde{q}^{(n-\frac{1}{n}) \frac{c_{\text{eff}}}{24}}, \quad (4.37)$$

where the coefficients are  $p_\rho = \frac{1}{3}, \forall \rho$ . Then it yields the following for SREE (3.11),

$$\begin{aligned} S(\mathcal{R}_\rho) &= \frac{c}{3} \log \left( \frac{L}{\epsilon} \right) + \log(g^2) + \log \left( \frac{d_\rho}{\sum d_\rho} \right), \quad \text{with, } g^2 = 3 \sqrt{\frac{1}{30}(5 - \sqrt{5})}, \quad d_\rho = 1 \\ &\rightarrow \frac{c}{3} \log \left( \frac{L}{\epsilon} \right) + \log(g^2) + \log \left( \frac{1}{|G|} \right), \quad |G| = \text{cardinality of } \mathbb{Z}_3. \end{aligned} \quad (4.38)$$

The quantum dimensions for the three lines are  $d_\rho = 1$ . In [141], the authors have obtained the same result using the form factor bootstrap method.

## 5 SREE in Non-Unitary Rational CFT

As we already discussed in the introduction, symmetry resolution has mainly been developed in unitary settings, i.e, for unitary fusion categories, modular data, and RCFTs. The non-unitary case remains largely unexplored. By bulk-boundary correspondence, unitary TQFTs

admit unitary boundary RCFT [98–103], and extending this logic beyond unitarity is a natural question [104]. Recent work shows that topological twists of certain  $3d \mathcal{N} = 4$  rank-zero (S-fold) SCFTs yield non-unitary TQFTs with modular data generalizing the Haagerup–Izumi constructions [105, 106]. Furthermore, modular data of non-unitary rational CFTs have been constructed using bulk-boundary correspondence and used the method of [142, 143]<sup>16</sup> to compute the characters<sup>17</sup> We begin our analysis by examining the simplest non-unitary RCFT, known as the Lee–Yang minimal model.

### 5.1 Lee–Yang Minimal Model $\mathcal{M}(5, 2)$ : a simplest example

The Lee–Yang minimal model is the simplest non-unitary rational CFT with central charge  $c = -\frac{22}{5}$ . It has two primaries with non-zero conformal dimension  $h = -\frac{1}{5}$ . This model possesses the Fibonacci fusion category symmetry, an example of non-invertible symmetry. The non-trivial fusion is given by

$$\Phi_2 \times \Phi_2 = \Phi_1 + \Phi_2 \quad (5.1)$$

where  $\Phi_1$  corresponds to the vacuum state and  $\Phi_2$  corresponds to a non-vacuum state, in this case, the non-vacuum state is the ground state  $|\Omega\rangle$ . For unitary theory, the vacuum state is the ground state, but not in non-unitary theory. It is a diagonal RCFT, and its modular S-matrix and characters are given by

$$S = \frac{2}{\sqrt{5}} \begin{pmatrix} -\sin\left(\frac{2\pi}{5}\right) & \sin\left(\frac{4\pi}{5}\right) \\ \sin\left(\frac{4\pi}{5}\right) & \sin\left(\frac{2\pi}{5}\right) \end{pmatrix}, \quad (5.2)$$

$$\chi_1(\tau) = q^{\frac{11}{60}} (1 + q^2 + q^3 + \dots), \quad (5.3)$$

$$\chi_2(\tau) = q^{-\frac{1}{60}} (1 + q + q^2 + \dots). \quad (5.4)$$

We want to study this Fibonacci fusion category symmetry-resolved entanglement entropy for this non-unitary minimal model by leveraging the techniques of BCFT as discussed earlier. The weakly symmetric Cardy boundary state and the annulus partition function in the open-string channel are given by

$$|\Phi_2\rangle = -i \left(1 - \frac{2}{\sqrt{5}}\right)^{\frac{1}{4}} |1\rangle\rangle + \frac{\sqrt{5 + 3\sqrt{5}}}{\sqrt[4]{10(5 + \sqrt{5})}} |2\rangle\rangle, \quad (5.5)$$

$$Z(q) = \chi_1(q) + \chi_2(q). \quad (5.6)$$

The Fibonacci fusion category  $\mathcal{C} = \{\Phi_1, \Phi_2\}$  has two elements; there are two irreps. Therefore, the reduced density matrix has two diagonal blocks. The action of  $\mathcal{C}$  on the primaries is given in the Table (4).

<sup>16</sup>For other interesting applications of this method please refer to [144, 145].

<sup>17</sup>One other method to compute characters of a rational CFT is known as MMS approach, by analyzing modular invariant linear differential equation (MLDE) [146–148]. For more details, readers are further referred to [149–151].

Defect line	$\Phi_1$	$\Phi_2$
$\mathcal{L}_{\Phi_1}$	1	1
$\mathcal{L}_{\Phi_2}$	$\frac{1-\sqrt{5}}{2}$	$\frac{1+\sqrt{5}}{2}$

**Table 4:** Action of the Fibonacci category on the primaries.

This action distinguishes two sectors. Therefore, the partition function is fully resolved, and in each block, there is a contribution from a single character. So, the symmetry-resolved partition functions are

$$Z(q^n, \mathcal{R}_1) = \frac{\chi_1(q^n)}{(Z(q))^n}, \quad Z(q^n, \mathcal{R}_2) = \frac{\chi_2(q^n)}{(Z(q))^n}. \quad (5.7)$$

Now, we can compute SREE. This is a non-unitary rational CFT; therefore, the leading contribution comes from the ground state rather than the vacuum. In this example,  $|\Omega\rangle = |\Phi_2\rangle\rangle$  is a ground state. Therefore,

$$\frac{Z(q^n, \mathcal{R}_1)}{Z^n(q, \mathcal{R}_1)} \underset{\tilde{q} \rightarrow 0}{\sim} \left( \sqrt{\frac{5-\sqrt{5}}{10}} \right)^{1-n} \tilde{q}^{(n-\frac{1}{n})\frac{c_{\text{eff}}}{24}} \quad (5.8)$$

and we get the SREE for the block  $\mathcal{R}_1$

$$S(\mathcal{R}_1) = \frac{c_{\text{eff}}}{3} \log\left(\frac{L}{\epsilon}\right) + \frac{1}{2} \log \frac{5-\sqrt{5}}{10} + \dots \quad (5.9)$$

where the constant term <sup>18</sup>

$$\frac{1}{2} \log \frac{5-\sqrt{5}}{10} = \log \left( \frac{d_{\mathcal{R}_1}}{\sum_{\mathcal{R}_i} d_{\mathcal{R}_i}} \right) + \log(\langle\langle \Phi_2 | \Omega \rangle \langle \Omega | \Phi_2 \rangle\rangle). \quad (5.10)$$

Here  $d_{\mathcal{R}_1} = 1$ ,  $\sum_{\mathcal{R}_i} d_{\mathcal{R}_i} = \frac{3+\sqrt{5}}{2}$ , and  $\log(\langle\langle \Phi_2 | \Omega \rangle \langle \Omega | \Phi_2 \rangle\rangle) = \log\left(\frac{5+3\sqrt{5}}{\sqrt{10(5+\sqrt{5})}}\right)$  corresponds to the Affleck-Ludwig boundary entropy [133]. Similarly, we have

$$S(\mathcal{R}_2) = \frac{c_{\text{eff}}}{3} \log\left(\frac{L}{\epsilon}\right) + \frac{1}{2} \log \frac{5+\sqrt{5}}{10} + \dots \quad (5.11)$$

and the constant term

$$\frac{1}{2} \log \frac{5+\sqrt{5}}{10} = \log \left( \frac{d_{\mathcal{R}_2}}{\sum_{\mathcal{R}_i} d_{\mathcal{R}_i}} \right) + \log(\langle\langle \Phi_2 | \Omega \rangle \langle \Omega | \Phi_2 \rangle\rangle) \quad (5.12)$$

where,  $d_{\mathcal{R}_2} = \frac{1+\sqrt{5}}{2}$  is the quantum dimension of  $\Phi_2$ .

<sup>18</sup>For non-unitary theory, bra and ket are not complex conjugate of each other in general. But, in our case it does and our results matches with those in [97]. We thank Yoshiki Fukusumi for pointing out thid connection to us.

## 5.2 The Haagerup Rational CFT $\mathcal{R}_{\kappa=3}$

We now turn to one of the central topics of our paper, the symmetry resolution of generalized Haagerup RCFTs. We begin with the simplest example,  $\mathcal{R}_{\kappa=3}$ , realized as the tensor product of the Virasoro minimal models  $\mathcal{M}(2, 5)$  and  $\mathcal{M}(3, 5)$ . The modular S-matrix is given by [105],

$$S = \begin{pmatrix} -a_0 & a_0 & a_3 & -a_3 & a_2 & -a_2 & a_2 & -a_2 \\ a_0 & a_0 & a_3 & a_3 & -a_2 & -a_2 & -a_2 & -a_2 \\ a_3 & a_3 & a_0 & a_0 & a_2 & a_2 & a_2 & a_2 \\ -a_3 & a_3 & a_0 & -a_0 & -a_2 & a_2 & -a_2 & a_2 \\ a_2 & -a_2 & a_2 & -a_2 & 2a_2 \cos\left(\frac{\pi}{5}\right) & 2a_2 \cos\left(\frac{2\pi}{5}\right) & 2a_2 \cos\left(\frac{3\pi}{5}\right) & 2a_2 \cos\left(\frac{4\pi}{5}\right) \\ -a_2 & -a_2 & a_2 & a_2 & 2a_2 \cos\left(\frac{2\pi}{5}\right) & 2a_2 \cos\left(\frac{4\pi}{5}\right) & 2a_2 \cos\left(\frac{6\pi}{5}\right) & 2a_2 \cos\left(\frac{8\pi}{5}\right) \\ a_2 & -a_2 & a_2 & -a_2 & 2a_2 \cos\left(\frac{3\pi}{5}\right) & 2a_2 \cos\left(\frac{6\pi}{5}\right) & 2a_2 \cos\left(\frac{9\pi}{5}\right) & 2a_2 \cos\left(\frac{12\pi}{5}\right) \\ -a_2 & -a_2 & a_2 & a_2 & 2a_2 \cos\left(\frac{4\pi}{5}\right) & 2a_2 \cos\left(\frac{8\pi}{5}\right) & 2a_2 \cos\left(\frac{12\pi}{5}\right) & 2a_2 \cos\left(\frac{16\pi}{5}\right) \end{pmatrix} \quad (5.13)$$

where,  $a_0 = \frac{1}{\sqrt{8(k+2)}} + \frac{1}{\sqrt{8(k-2)}}$ ,  $a_1 = \frac{1}{\sqrt{2(k-2)}}$ ,  $a_2 = \frac{1}{\sqrt{2(k+2)}}$ ,  $a_3 = \frac{1}{\sqrt{8(k-2)}} - \frac{1}{\sqrt{8(k+2)}}$ , with  $k = 3$ . The full fusion can be immediately found by the Verlinde formula. However, by carefully inspecting the full fusion one can find that the following primaries  $\Phi_1, \Phi_4, \Phi_5, \Phi_7$  form a sub-fusion. The sub-fusion is given by,

$$\begin{aligned} \Phi_4 \times \Phi_4 &= \Phi_1 + \Phi_4 + \Phi_5 + \Phi_7, \\ \Phi_5 \times \Phi_4 &= \Phi_4 + \Phi_7, \\ \Phi_5 \times \Phi_5 &= \Phi_1 + \Phi_5, \\ \Phi_7 \times \Phi_4 &= \Phi_4 + \Phi_5, \\ \Phi_7 \times \Phi_5 &= \Phi_4, \\ \Phi_7 \times \Phi_7 &= \Phi_1 + \Phi_7. \end{aligned} \quad (5.14)$$

The sub-fusion category has four elements and, accordingly, four irreducible representations  $\{\mathcal{R}_i\}_{i=1}^6$ . Consequently, the reduced density matrix of subsystem  $A$ ,  $\rho_A$ , decomposes into four distinct (mutually orthogonal) blocks, each carrying a unique character. However, the attainable resolution depends on whether the defect lines act distinctly on the primaries: primaries with identical defect action remain in the same block. To proceed further, we investigate the action of (topological) defects on the primary fields. We carry out our analysis using the diagonal RCFT associated with the  $\mathcal{R}_{\kappa=3}$  modular data, where primaries and topological defects are in one-to-one correspondence. Equivalently, each defect  $\mathcal{L}_a$  (labeled by a primary  $a$ ) acts diagonally on primaries:

$$\mathcal{L}_a \Phi_i = \lambda_a(i) \Phi_i, \quad \lambda_a(i) = \frac{S_{ai}}{S_{1i}}, \quad (5.15)$$

where  $S$  is the modular  $S$ -matrix. Table (5) summarizes the action of defects on the primaries.

	$\Phi_1$	$\Phi_4$	$\Phi_5$	$\Phi_7$
$\mathcal{L}_1$	1	1	1	1
$\mathcal{L}_4$	$\frac{1}{2}(3 - \sqrt{5})$	$\frac{1}{2}(\sqrt{5} + 3)$	-1	-1
$\mathcal{L}_5$	$\frac{1}{2}(1 - \sqrt{5})$	$\frac{1}{2}(\sqrt{5} + 1)$	$\frac{1}{2}(\sqrt{5} + 1)$	$\frac{1}{2}(1 - \sqrt{5})$
$\mathcal{L}_7$	$\frac{1}{2}(1 - \sqrt{5})$	$\frac{1}{2}(\sqrt{5} + 1)$	$\frac{1}{2}(1 - \sqrt{5})$	$\frac{1}{2}(\sqrt{5} + 1)$

**Table 5:** Eigenvalues  $\lambda_{\mathcal{L}_a}(i)$  for the action of defect  $\mathcal{L}_a$  on primary  $\Phi_i$  in a diagonal RCFT, with  $\lambda_a(i) = \frac{S_{ai}}{S_{1i}}$ .

In this non-unitary RCFT the state of lowest conformal weight (the ‘‘ground state’’ for thermodynamic purposes) is  $|\Phi_3\rangle$ , not the identity. Consequently, the quantum dimensions of the topological defect lines  $\mathcal{L}_a$  are evaluated relative to  $|\Phi_3\rangle$  via the modular  $S$ -matrix:

$$d_{\mathcal{L}_a} = \frac{S_{a3}}{S_{13}}. \quad (5.16)$$

For the defects of interest, we obtain

$$d_{\mathcal{L}_1} = 1, \quad d_{\mathcal{L}_4} = \frac{1}{2}(\sqrt{5} + 3), \quad d_{\mathcal{L}_5} = \frac{1}{2}(\sqrt{5} + 1), \quad d_{\mathcal{L}_7} = \frac{1}{2}(\sqrt{5} + 1). \quad (5.17)$$

To compute the annulus partition function, we choose the (weakly) symmetric boundary state  $\|\Phi_4\rangle\rangle$ . The closed-string channel amplitude is then

$$Z(\tilde{q}) = \langle\langle \Phi_4 | \tilde{q}^{L_0 - \frac{c}{24}} | \Phi_4 \rangle\rangle, \quad (5.18)$$

where  $\tilde{q}$  is the modular parameter in the closed channel. The partition function in (5.18) can be computed by expanding the boundary Cardy states in terms of Ishibashi states as,

$$\|B_i\rangle\rangle = \sum_j \frac{S_{ij}}{\sqrt{S_{1j}}} |j\rangle\rangle, \quad \text{with, } B_i = \Phi_4, \quad (5.19)$$

where  $|j\rangle\rangle$ 's are the Ishibashi states and using the following property of Ishibashi states:  $\langle\langle i | \tilde{q}^{L_0 - \frac{c}{24}} | j \rangle\rangle = \chi_i(\tilde{q}) \delta_{ij}$ . In the open string channel, the partition function takes the following form (3.5),

$$Z(q) = \chi_1(q) + \chi_4(q) + \chi_5(q) + \chi_7(q). \quad (5.20)$$

As shown in the Table (5), the action of defects  $\mathcal{L}_a$  is clearly different on the primaries, hence we have four irreducible blocks. The leading contribution to the partition function at  $\tilde{q} \rightarrow 0$  limit is given by,

$$\begin{aligned} Z(q^n, \Phi_1) &\sim \frac{5 - \sqrt{5}}{10\sqrt{2}} \chi_3(\tilde{q}^{\frac{1}{n}}), & Z(q^n, \Phi_4) &\sim \frac{1}{2} \sqrt{\frac{3}{5} + \frac{1}{\sqrt{5}}} \chi_3(\tilde{q}^{\frac{1}{n}}), & Z(q^n, \Phi_5) &\sim \frac{1}{\sqrt{10}} \chi_3(\tilde{q}^{\frac{1}{n}}), \\ Z(q^n, \Phi_7) &\sim \frac{1}{\sqrt{10}} \chi_3(\tilde{q}^{\frac{1}{n}}). \end{aligned} \quad (5.21)$$

Therefore, the SREE for the first irreducible block is given by,

$$S(\mathcal{R}_1) = \frac{c_{\text{eff}}}{3} \log\left(\frac{L}{\epsilon}\right) + \log\left(\frac{5 - \sqrt{5}}{10\sqrt{2}}\right) + \dots \quad (5.22)$$

Therefore the consistency condition from (3.9) is the following,

$$\log\left(\frac{5 - \sqrt{5}}{10\sqrt{2}}\right) \stackrel{?}{=} \log(g^2) + \log\left(\frac{d_\rho N_{\rho B_1}^{B_2}}{d(B_1 \otimes B_2)}\right). \quad (5.23)$$

Now computing the RHS independently, we find,

$$g^2 = |\langle\langle\Phi_4|\Omega\rangle\rangle|^2 = \sqrt{\frac{2}{5}} + \frac{1}{\sqrt{2}}, \quad \log\left(\frac{d_\rho N_{\rho B_1}^{B_2}}{d(B_1 \otimes B_2)}\right) = \frac{1}{2} (7 - 3\sqrt{5}). \quad (5.24)$$

Putting (5.24) in (5.23), one can show that the equality in (3.9) (or more generally (3.12)) indeed holds. Note that we choose the boundary as weakly symmetric, for which we notice that  $d(B_1 \otimes B_2) = \sum_\rho d_{\mathcal{L}_\rho}$ , and the expression for the entanglement entropy reduces to (3.11).

Next, we turn to the example of  $\mathcal{R}_{k=4}$  [105], where several subtleties arise. In particular, the relevant sub-fusion ring exhibits non-trivial multiplicities, and we find that the standard methods do not yield a complete symmetry resolution. We make a detailed comment on that.

### 5.3 The Haagerup Rational CFT $\mathcal{R}_{\kappa=4}$

Haagerup  $\mathcal{R}_{\kappa=4}$  is also a non-unitary rational conformal field theory with ten primaries with central charge  $c = -11$  and conformal dimensions are  $h_i = \{\frac{3}{2}, -\frac{1}{2}, 0, -\frac{3}{8}, -\frac{11}{24}, -\frac{1}{3}, -\frac{1}{8}, \frac{1}{6}, \frac{13}{24}\}$  [105], which can also be realized as non-unitary super-Virasoro minimal model  $\mathcal{SM}(2, 12)$ . The modular S-matrix by which these characters transform under  $\tau \rightarrow -\frac{1}{\tau}$  is given by [105],

$$S = \begin{pmatrix} a_0 & a_0 & a_3 & a_3 & -a_1 & a_2 & -a_2 & a_2 & -a_2 & a_2 \\ a_0 & a_0 & a_3 & a_3 & a_1 & -a_2 & -a_2 & -a_2 & -a_2 & -a_2 \\ a_3 & a_3 & a_0 & a_0 & a_1 & a_2 & a_2 & a_2 & a_2 & a_2 \\ a_3 & a_3 & a_0 & a_0 & -a_1 & -a_2 & a_2 & -a_2 & a_2 & -a_2 \\ -a_1 & a_1 & a_1 & -a_1 & 2a_1 \cos\left(\frac{\pi}{2}\right) & 0 & 0 & 0 & 0 & 0 \\ a_2 & -a_2 & a_2 & -a_2 & 0 & 2a_2 \cos\left(\frac{\pi}{6}\right) & 2a_2 \cos\left(\frac{2\pi}{6}\right) & 2a_2 \cos\left(\frac{3\pi}{6}\right) & 2a_2 \cos\left(\frac{4\pi}{6}\right) & 2a_2 \cos\left(\frac{5\pi}{6}\right) \\ -a_2 & -a_2 & a_2 & a_2 & 0 & 2a_2 \cos\left(\frac{2\pi}{6}\right) & 2a_2 \cos\left(\frac{4\pi}{6}\right) & 2a_2 \cos\left(\frac{6\pi}{6}\right) & 2a_2 \cos\left(\frac{8\pi}{6}\right) & 2a_2 \cos\left(\frac{10\pi}{6}\right) \\ a_2 & -a_2 & a_2 & -a_2 & 0 & 2a_2 \cos\left(\frac{3\pi}{6}\right) & 2a_2 \cos\left(\frac{6\pi}{6}\right) & 2a_2 \cos\left(\frac{9\pi}{6}\right) & 2a_2 \cos\left(\frac{12\pi}{6}\right) & 2a_2 \cos\left(\frac{15\pi}{6}\right) \\ -a_2 & -a_2 & a_2 & a_2 & 0 & 2a_2 \cos\left(\frac{4\pi}{6}\right) & 2a_2 \cos\left(\frac{8\pi}{6}\right) & 2a_2 \cos\left(\frac{12\pi}{6}\right) & 2a_2 \cos\left(\frac{16\pi}{6}\right) & 2a_2 \cos\left(\frac{20\pi}{6}\right) \\ a_2 & -a_2 & a_2 & -a_2 & 0 & 2a_2 \cos\left(\frac{5\pi}{6}\right) & 2a_2 \cos\left(\frac{10\pi}{6}\right) & 2a_2 \cos\left(\frac{15\pi}{6}\right) & 2a_2 \cos\left(\frac{20\pi}{6}\right) & 2a_2 \cos\left(\frac{25\pi}{6}\right) \end{pmatrix} \quad (5.25)$$

where,  $a_0 = \frac{1}{\sqrt{8(\kappa-2)}} + \frac{1}{\sqrt{8(\kappa+2)}}$ ,  $a_1 = \frac{1}{\sqrt{2(\kappa-2)}}$ ,  $a_2 = \frac{1}{\sqrt{2(\kappa+2)}}$ ,  $a_3 = \frac{1}{\sqrt{8(\kappa-2)}} - \frac{1}{\sqrt{8(\kappa+2)}}$ ,  $\kappa = 4$ . Therefore, we can compute the fusion rule of the primaries, and we have noticed that there is a sub-fusion algebra generated by  $\mathcal{C} = \{\Phi_1, \Phi_2, \Phi_3, \Phi_4, \Phi_7, \Phi_9\}$ .

$$\begin{aligned}
\Phi_2 \times \Phi_2 &= \Phi_1, & \Phi_7 \times \Phi_2 &= \Phi_9, \\
\Phi_3 \times \Phi_2 &= \Phi_4, & \Phi_7 \times \Phi_3 &= \Phi_3 + \Phi_4 + \Phi_7, \\
\Phi_3 \times \Phi_3 &= \Phi_1 + \Phi_3 + \Phi_4 + \Phi_7 + \Phi_9, & \Phi_7 \times \Phi_4 &= \Phi_3 + \Phi_4 + \Phi_9, \\
\Phi_4 \times \Phi_2 &= \Phi_3, & \Phi_7 \times \Phi_7 &= \Phi_1 + \Phi_3 + \Phi_9, \\
\Phi_4 \times \Phi_3 &= \Phi_2 + \Phi_3 + \Phi_4 + \Phi_7 + \Phi_9, & \Phi_9 \times \Phi_2 &= \Phi_7, \\
\Phi_4 \times \Phi_4 &= \Phi_1 + \Phi_3 + \Phi_4 + \Phi_7 + \Phi_9, & \Phi_9 \times \Phi_3 &= \Phi_3 + \Phi_4 + \Phi_9, \\
\Phi_5 \times \Phi_2 &= \Phi_5, & \Phi_9 \times \Phi_4 &= \Phi_3 + \Phi_4 + \Phi_7, \\
& & \Phi_9 \times \Phi_7 &= \Phi_2 + \Phi_4 + \Phi_7, \\
& & \Phi_9 \times \Phi_9 &= \Phi_1 + \Phi_3 + \Phi_9.
\end{aligned} \tag{5.26}$$

We also notice that the boundary state  $\|\Phi_5\rangle\rangle$  is weakly symmetric under this fusion category  $\mathcal{C}$ .

$$\begin{aligned}
\mathcal{L}_{\Phi_1}\|\Phi_5\rangle\rangle &= \|\Phi_5\rangle\rangle, \\
\mathcal{L}_{\Phi_2}\|\Phi_5\rangle\rangle &= \|\Phi_5\rangle\rangle, \\
\mathcal{L}_{\Phi_3}\|\Phi_5\rangle\rangle &= \|\Phi_5\rangle\rangle \oplus \|\Phi_5\rangle\rangle \oplus \|\Phi_6\rangle\rangle \oplus \|\Phi_8\rangle\rangle \oplus \|\Phi_{10}\rangle\rangle, \\
\mathcal{L}_{\Phi_4}\|\Phi_5\rangle\rangle &= \|\Phi_5\rangle\rangle \oplus \|\Phi_5\rangle\rangle \oplus \|\Phi_6\rangle\rangle \oplus \|\Phi_8\rangle\rangle \oplus \|\Phi_{10}\rangle\rangle, \\
\mathcal{L}_{\Phi_7}\|\Phi_5\rangle\rangle &= \|\Phi_5\rangle\rangle \oplus \|\Phi_5\rangle\rangle \oplus \|\Phi_6\rangle\rangle \oplus \|\Phi_8\rangle\rangle \oplus \|\Phi_{10}\rangle\rangle, \\
\mathcal{L}_{\Phi_9}\|\Phi_5\rangle\rangle &= \|\Phi_5\rangle\rangle \oplus \|\Phi_5\rangle\rangle \oplus \|\Phi_6\rangle\rangle \oplus \|\Phi_8\rangle\rangle \oplus \|\Phi_{10}\rangle\rangle.
\end{aligned} \tag{5.27}$$

The untwisted partition function in the closed string channel and open string channel are given respectively by,

$$\begin{aligned}
Z(q^n) &= \frac{3}{3+\sqrt{3}} \chi_1(\tilde{q}^{\frac{1}{n}}) + \frac{3}{3+\sqrt{3}} \chi_2(\tilde{q}^{\frac{1}{n}}) + \frac{3}{3-\sqrt{3}} \chi_3(\tilde{q}^{\frac{1}{n}}) + \frac{3}{3-\sqrt{3}} \chi_4(\tilde{q}^{\frac{1}{n}}), \\
&= \chi_1(q^n) + \chi_2(q^n) + 2\chi_3(q^n) + 2\chi_4(q^n) + \chi_7(q^n) + \chi_9(q^n).
\end{aligned} \tag{5.28}$$

Note that the chosen weakly symmetric boundary state,  $\|B\rangle\rangle = \|\Phi_5\rangle\rangle$  does not belong to the sub-fusion. However, from the fusion table, one can immediately see that  $B \otimes B$  again generates all the elements of the sub-fusion. From Table (6), it is clear that the actions of the six defect lines are the same for the following blocks:  $\{\Phi_1, \Phi_2\}$ ,  $\{\Phi_3, \Phi_4\}$ ,  $\{\Phi_7, \Phi_9\}$ . Therefore, there will be three blocks (reducible) to be resolved.

Defect line/Bulk primary	$\Phi_1$	$\Phi_2$	$\Phi_3$	$\Phi_4$	$\Phi_5$	$\Phi_6$	$\Phi_7$	$\Phi_8$	$\Phi_9$	$\Phi_{10}$
$\mathcal{L}_{\Phi_1}$	1	1	1	1	1	1	1	1	1	1
$\mathcal{L}_{\Phi_2}$	1	1	1	1	-1	-1	1	-1	1	-1
$\mathcal{L}_{\Phi_3}$	$2 - \sqrt{3}$	$2 - \sqrt{3}$	$2 + \sqrt{3}$	$2 + \sqrt{3}$	-1	1	-1	1	-1	1
$\mathcal{L}_{\Phi_4}$	$2 - \sqrt{3}$	$2 - \sqrt{3}$	$2 + \sqrt{3}$	$2 + \sqrt{3}$	1	-1	-1	-1	-1	-1
$\mathcal{L}_{\Phi_7}$	$1 - \sqrt{3}$	$1 - \sqrt{3}$	$1 + \sqrt{3}$	$1 + \sqrt{3}$	0	1	1	-2	1	1
$\mathcal{L}_{\Phi_9}$	$1 - \sqrt{3}$	$1 - \sqrt{3}$	$1 + \sqrt{3}$	$1 + \sqrt{3}$	0	-1	1	2	1	-1

**Table 6:** Action of the defect lines on primaries.

The leading contribution to the partition function at  $\tilde{q} \rightarrow 0$  limit is given by,

$$Z(q^n, \mathcal{R}_1) \stackrel{\tilde{q} \rightarrow 0}{\sim} \frac{1}{6} (3 - \sqrt{3}) \chi_3(\tilde{q}^{\frac{1}{n}}), \quad Z(q^n, \mathcal{R}_2) \stackrel{\tilde{q} \rightarrow 0}{\sim} \left(1 + \frac{1}{\sqrt{3}}\right) \chi_3(\tilde{q}^{\frac{1}{n}}), \quad Z(q^n, \mathcal{R}_3) = \frac{1}{\sqrt{3}} \chi_3(\tilde{q}). \quad (5.29)$$

The *partially* resolved entanglement entropy for each block is given by,

$$\begin{aligned} S(\mathcal{R}_1) &= \frac{c_{\text{eff}}}{3} \log\left(\frac{L}{\epsilon}\right) + \log\left(\frac{1}{6} (3 - \sqrt{3})\right), \\ S(\mathcal{R}_2) &= \frac{c_{\text{eff}}}{3} \log\left(\frac{L}{\epsilon}\right) + \log\left(1 + \frac{1}{\sqrt{3}}\right), \\ S(\mathcal{R}_3) &= \frac{c_{\text{eff}}}{3} \log\left(\frac{L}{\epsilon}\right) + \log\left(\frac{1}{\sqrt{3}}\right). \end{aligned} \quad (5.30)$$

Now we ask the same question as before by making a comparison with (3.9),

$$\begin{aligned} \text{block-1: } & \log\left(\frac{1}{6} (3 - \sqrt{3})\right) \stackrel{?}{=} \log(g^2) + \log\left(\frac{d_\rho N_{\rho B_1}^{B_2}}{d(B_1 \otimes B_2)}\right), \quad \rho \in \mathcal{R}_1, \\ \text{block-2: } & \log\left(1 + \frac{1}{\sqrt{3}}\right) \stackrel{?}{=} \log(g^2) + \log\left(\frac{d_\rho N_{\rho B_1}^{B_2}}{d(B_1 \otimes B_2)}\right), \quad \rho \in \mathcal{R}_2, \\ \text{block-3: } & \log\left(\frac{1}{\sqrt{3}}\right) \stackrel{?}{=} \log(g^2) + \log\left(\frac{d_\rho N_{\rho B_1}^{B_2}}{d(B_1 \otimes B_2)}\right), \quad \rho \in \mathcal{R}_3. \end{aligned} \quad (5.31)$$

Again, independent computation shows,

$$\begin{aligned} g^2 &= |\langle\langle \Phi_5 | \Omega \rangle\rangle|^2 = \frac{1}{2} (\sqrt{3} + 3), \\ \frac{\sum_{i \in \rho} d_i N_{i B_1}^{B_2}}{d(B_1 \otimes B_2)} &= \left\{ \frac{2}{(\sqrt{3} + 3)^2}, \frac{2}{3}, \left(\frac{1}{\sqrt{3}} - \frac{1}{3}\right) \right\}, \quad \forall i \in \rho = 1, 2, 3 \quad (\text{respectively}). \end{aligned} \quad (5.32)$$

Substituting (5.32) into (5.31) confirms that the equality of (3.9) remains valid. However, (3.11) does not apply here: the multiplicity-free assumption is violated, the fusion exhibits

nontrivial multiplicities, and also the resulting blocks are not made up from single characters. Apart from that, one may notice that the *defect lines discussed above do not fully resolve the symmetry sector*. Can we further refine the decomposition into smaller irreducible blocks? The answer is *to some extent*-yes, thanks to [84].

**Prescription. Refinement via an auxiliary defect.** Introduce an additional defect line associated with the boundary state  $\|\Phi_5\rangle\rangle$ , denoted by  $\mathcal{L}_{\Phi_5}$ , and examine its action on the primaries of the chosen subcategory. If this defect acts differently on the primaries within a single block  $\mathcal{R}_i$ , that is, if the images/eigenvalues under  $\mathcal{L}_{\Phi_5}$  are not identical, then  $\mathcal{R}_i$  splits into two irreducible blocks; otherwise, no further refinement occurs. Applying this prescription to our case, the action of  $\mathcal{L}_{\Phi_5}$  separates the primaries in the first two blocks, thereby splitting each into two irreducible blocks, while it fails to further decompose the third block. Consequently, *we obtain five blocks in total—four irreducible and one remaining reducible*. A straightforward calculation, in the same spirit as above, once again confirms (3.9).

#### 5.4 The Haagerup Rational CFT $\mathcal{R}_{\kappa=5}$

Finally, we consider another example of a generalized Haagerup fusion category, namely  $\mathcal{R}_{\kappa=5}$  [105]. The theory possesses six integrable highest-weight representations labeled by spins,  $j = 0, \frac{1}{2}, 1, \frac{3}{2}, 2, \frac{5}{2}$ . Below, we discuss the fusion of primaries in the fusion category. We again find that a sub-fusion exists and is given by,

$$\begin{aligned}
\Phi_4 \times \Phi_4 &= \Phi_1 + \Phi_4 + \Phi_5 + \Phi_7 + \Phi_9 + \Phi_{11}, & \Phi_7 \times \Phi_7 &= \Phi_1 + \Phi_5 + \Phi_7 + \Phi_9, \\
\Phi_4 \times \Phi_5 &= \Phi_4 + 2\Phi_5 + \Phi_7 + \Phi_9 + \Phi_{11}, & \Phi_7 \times \Phi_9 &= \Phi_4 + \Phi_5 + \Phi_7, \\
\Phi_4 \times \Phi_7 &= \Phi_4 + \Phi_5 + \Phi_9 + \Phi_{11}, & \Phi_7 \times \Phi_{11} &= \Phi_4 + \Phi_5 + \Phi_{11}, \\
\Phi_4 \times \Phi_9 &= \Phi_4 + \Phi_5 + \Phi_7 + \Phi_{11}, & \Phi_9 \times \Phi_9 &= \Phi_1 + \Phi_5 + \Phi_9 + \Phi_{11}, \\
\Phi_4 \times \Phi_{11} &= \Phi_4 + \Phi_5 + \Phi_7 + \Phi_9, & \Phi_9 \times \Phi_{11} &= \Phi_4 + \Phi_5 + \Phi_9, \\
\Phi_5 \times \Phi_5 &= \Phi_1 + 2\Phi_4 + 2\Phi_5 + \Phi_7 + \Phi_9 + \Phi_{11}, & \Phi_{11} \times \Phi_{11} &= \Phi_1 + \Phi_5 + \Phi_7 + \Phi_{11}. \\
\Phi_5 \times \Phi_7 &= \Phi_4 + \Phi_5 + \Phi_7 + \Phi_9 + \Phi_{11}, \\
\Phi_5 \times \Phi_9 &= \Phi_4 + \Phi_5 + \Phi_7 + \Phi_9 + \Phi_{11}, \\
\Phi_5 \times \Phi_{11} &= \Phi_4 + \Phi_5 + \Phi_7 + \Phi_9 + \Phi_{11},
\end{aligned}$$

Defect line/Bulk primary	$\Phi_1$	$\Phi_4$	$\Phi_5$	$\Phi_7$	$\Phi_9$	$\Phi_{11}$
$\mathcal{L}_{\Phi_1}$	1	1	1	1	1	1
$\mathcal{L}_{\Phi_4}$	$\frac{5-\sqrt{21}}{2}$	$\frac{5+\sqrt{21}}{2}$	1	-1	-1	-1
$\mathcal{L}_{\Phi_5}$	$\frac{7-\sqrt{21}}{2}$	$\frac{7+\sqrt{21}}{2}$	-1	0	0	0
$\mathcal{L}_{\Phi_7}$	$\frac{3-\sqrt{21}}{2}$	$\frac{3+\sqrt{21}}{2}$	0	$2 \cos\left(\frac{\pi}{7}\right)$	$2 \sin\left(\frac{\pi}{14}\right)$	$-2 \sin\left(\frac{3\pi}{14}\right)$
$\mathcal{L}_{\Phi_9}$	$\frac{3-\sqrt{21}}{2}$	$\frac{3+\sqrt{21}}{2}$	0	$2 \sin\left(\frac{\pi}{14}\right)$	$-2 \sin\left(\frac{3\pi}{14}\right)$	$2 \cos\left(\frac{\pi}{7}\right)$
$\mathcal{L}_{\Phi_{11}}$	$\frac{3-\sqrt{21}}{2}$	$\frac{3+\sqrt{21}}{2}$	0	$-2 \sin\left(\frac{3\pi}{14}\right)$	$2 \cos\left(\frac{\pi}{7}\right)$	$2 \sin\left(\frac{\pi}{14}\right)$

**Table 7:** Action of the defect lines on primaries.

The sub-fusion category contains six elements,  $\mathcal{C} = \{\Phi_1, \Phi_4, \Phi_5, \Phi_7, \Phi_9, \Phi_{11}\}$ , so it has six irreducible representations,  $\mathcal{R}_i$ . We can see from the Table (7) that the action of  $\mathcal{C}$  on all the primaries is distinct. Therefore, we conclude that a single character will contribute in each representation/block in the reduced density matrix  $\rho_A$ , namely, if we take  $|\Phi_4\rangle\rangle$  as a weakly symmetric boundary state, we have the following partition function and symmetry-resolved partition functions in the open-string channel respectively,

$$Z(q) = \chi_1(q) + \chi_4(q) + \chi_5(q) + \chi_7(q) + \chi_9(q) + \chi_{11}(q) \quad (5.33)$$

and,

$$\begin{aligned} Z(q^n, \mathcal{R}_1) &= \frac{\chi_1(q^n)}{(Z(q))^n}, & Z(q^n, \mathcal{R}_2) &= \frac{\chi_4(q^n)}{(Z(q))^n}, & Z(q^n, \mathcal{R}_3) &= \frac{\chi_5(q^n)}{(Z(q))^n}, \\ Z(q^n, \mathcal{R}_4) &= \frac{\chi_7(q^n)}{(Z(q))^n}, & Z(q^n, \mathcal{R}_5) &= \frac{\chi_9(q^n)}{(Z(q))^n}, & Z(q^n, \mathcal{R}_6) &= \frac{\chi_{11}(q^n)}{(Z(q))^n}. \end{aligned} \quad (5.34)$$

This is a non-unitary rational CFT; therefore leading contribution comes from the ground state rather than the vacuum in *overset* $\tilde{q} \rightarrow 0$ . In this example,  $|\Phi_3\rangle$  is a ground state. Finally, we get the following expressions for the SREE for the different blocks.

$$S_n(\mathcal{R}_1) = \frac{c_{\text{eff}}}{3} \log\left(\frac{L}{\epsilon}\right) + \log \frac{1}{2} \left( \frac{1}{\sqrt{6}} - \frac{1}{\sqrt{14}} \right) + \dots \quad (5.35)$$

where the constant term

$$\log \frac{1}{2} \left( \frac{1}{\sqrt{6}} - \frac{1}{\sqrt{14}} \right) = \log \left( \frac{d_{\mathcal{R}_1}}{\sum_{\mathcal{R}_i} d_{\mathcal{R}_i}} \right) + \log(\langle\langle \Phi_4 | \Omega \rangle \langle \Omega | \Phi_4 \rangle\rangle). \quad (5.36)$$

Here  $d_{\mathcal{R}_1} = 1$ ,  $\sum_{\mathcal{R}_i} d_{\mathcal{R}_i} = \frac{23+5\sqrt{21}}{2}$ , and  $\log(\langle\langle \Phi_4 | \Omega \rangle \langle \Omega | \Phi_4 \rangle\rangle) = \frac{1}{2} \log \left( \frac{55}{42} + 2\sqrt{\frac{3}{7}} \right)$  corresponds to the Affleck-Ludwig boundary entropy [133]. Similarly, we have

$$S_n(\mathcal{R}_2) = \frac{c_{\text{eff}}}{6} \left( \frac{n+1}{n} \right) \log\left(\frac{L}{\epsilon}\right) + \log \frac{1}{2} \left( \sqrt{\frac{5+\sqrt{21}}{21}} \right) + \dots \quad (5.37)$$

and the constant term

$$\log \frac{1}{2} \left( \sqrt{\frac{5 + \sqrt{21}}{21}} \right) = \log \left( \frac{d_{\mathcal{R}_2}}{\sum_{\mathcal{R}_i} d_{\mathcal{R}_i}} \right) + \log(\langle\langle \Phi_4 \| \Omega \rangle \langle \Omega \| \Phi_4 \rangle\rangle) \quad (5.38)$$

where,  $d_{\mathcal{R}_2} = \frac{5 + \sqrt{21}}{2}$  is the quantum dimension of  $\mathcal{L}_{\Phi_4}$ .

## 6 Summary and Conclusion

In this work, we have investigated the symmetry-resolved entanglement entropy (SREE) in  $(1+1)$ -dimensional critical systems possessing *categorical* symmetries. Our interest has been in a broad class of rational conformal field theories (RCFTs), including examples that are (1) non-unitary, (2) non-diagonal, and (3) exhibit multiplicities in their fusion rules, for which symmetry resolution is substantially more intricate than in the conventional group-like or unitary diagonal cases. The general motivation for our study comes from the ongoing effort to understand how entanglement structures encode internal and categorical symmetry data in quantum field theories. In particular, recent developments in Symmetry Topological Field Theory (SymTFT) [21, 152–158] and the study of defect networks provide a powerful framework to interpret charges and sectors in RCFTs. However, explicit computations of SREE in non-unitary and non-diagonal theories, especially those with non-group-like symmetry categories, have remained limited. This work aims to fill that gap.

### Summary of Results.

Our analysis and main results may be summarized as follows:

- **General Framework for Categorical Symmetry Resolution.** We first discussed the role of boundary conditions in symmetry resolution and introduced a general prescription of computing SREE. Inspired by [1], we provide a general formula for the SREE that uniformly applies to symmetric (weakly or strongly) and cloaking boundary conditions, as well as to fusion rings with multiplicities, without invoking any SymTFT construction. Our approach relies solely on a purely two-dimensional RCFT analysis. This formalism applies not only to weakly and strongly symmetric boundary conditions, but also to the more subtle *cloaking* boundary conditions, and it naturally accommodates fusion categories with multiplicities. We demonstrated that the resulting formula is universally applicable across a wide range of RCFTs, irrespective of unitarity or diagonality.
- **Replica Computations, Universal Scaling, and Boundary entropy.** We carried out explicit replica computations of the von Neumann entropy associated with each symmetry sector, identifying both the universal leading contributions and the subleading corrections associated with boundary entropy. For several unitary and non-unitary models, we evaluated the SREE via first principles and made a connection with the

generalized Affleck–Ludwig boundary entropy formula. We began with the Tambara–Yamagami (TY) fusion category structure in the Ising CFT, where the absence of weakly/strongly symmetric boundary conditions necessitates cloaking boundary states. We also analyze the SREE for the tetracritical Ising model. Interestingly, in this case, we found that, there were two natural choices of sub-fusion categories. For the larger sub-fusion category we find that no weakly symmetric boundary state exists, but we can still perform the resolution using an appropriate cloaking boundary state. In contrast, for the smaller sub-fusion category, a weakly symmetric boundary state was available. We subsequently turned to non-diagonal RCFTs. In the  $SU(2)_{10}$  theory with  $E_6$  modular invariant, we showed that symmetry resolution with respect to the  $\frac{1}{2}E_6$  fusion ring fails: although one may choose a weakly symmetric boundary state  $\|Y\rangle\rangle$ , the open-channel spectrum contains primaries that do not appear in the  $E_6$  fusion ring. Therefore, the resolution is *ambiguous* and no consistent sector decomposition exists. By contrast, for the three-state Potts model, we demonstrated that symmetry resolution with respect to the  $\mathbb{Z}_3$  symmetry is possible, provided one selects an appropriate weakly symmetric boundary condition.

- ***Non-Unitary Symmetry Resolution and Generalized Haagerup RCFTs.*** We then studied the symmetry resolution in non-unitary settings. As a starting point, we computed the SREE for the Lee–Yang minimal model. Following this, we addressed generalized Haagerup RCFTs, whose modular data encode non-group-like categorical symmetries and which may not necessarily admit a well-defined VOA realization. This makes the implementation of boundary-based SREE calculations particularly subtle. We reviewed the modular and categorical data of the Haagerup family  $\mathcal{R}_k$ , discussed the structure of simple objects and fusion channels, and emphasized the non-invertible symmetry interpretation. By carefully identifying admissible Cardy boundary states, we explicitly computed the symmetry-resolved entanglement entropies for  $\mathcal{R}_{k=3,4,5}$ . Our findings show that with an appropriate choice of weakly symmetric boundary conditions, *full symmetry-sector resolution* is achievable for  $\mathcal{R}_3$  and  $\mathcal{R}_5$ . However, for  $\mathcal{R}_4$ , a complete resolution is *not* possible when restricting to defect subfusion sectors alone. We demonstrated that introducing boundary defects allows one to improve and, in some cases, complete the resolution.

***Outlook and open problem*** There are several interesting future directions possible. We list a few of them below. It is highly compelling to consider extending these computations beyond the realm of rational conformal field theories (RCFTs). *This naturally raises several fundamental questions, for instance, whether the existence of a vertex operator algebra (VOA) is a necessary condition for the existence of a corresponding symmetry topological field theory (SymTFT)?* A particularly promising direction is to refine and generalize the existing framework so as to address the challenges of symmetry resolution in non-diagonal RCFTs, where modular invariants and fusion structures become considerably more intricate.

In addition to this, our current analysis has primarily focused on line operators, which correspond to 0-form defects. A natural next step would be to explore the broader landscape of higher-form defects, such as condensation or domain-wall defects, which play a crucial role in the categorical and geometric understanding of symmetry breaking and topological phase transitions. Another significant avenue of investigation lies in the explicit computation of the anomaly inflow action. Determining this action would allow one to identify and characterize the electric and magnetic defect lines, *along with their associated bulk linkings*. Such an analysis could shed light on the interplay between boundary symmetries and bulk topological data, ultimately contributing to a deeper understanding of the correspondence between conformal and topological field theories.

## Acknowledgments

We would like to thank Brandon Rayhaun for detailed comments on the previous version of the manuscript. A.B and J.S would also like to thank Arpit Das and Thomas Quella for discussions on related topics and comments on some parts of the draft, as well as making us aware of the upcoming work [85]. J.S is indebted to Suresh Govindarajan, Chethan N. Gowdigere, and Akhila S. for useful discussions. S.G would like to thank Jayashish Das for discussion on related topic. S.G (PMRF ID: 1702711) and S.P (PMRF ID: 1703278) is supported by the Prime Minister’s Research Fellowship of the Government of India. S.G would like to thank Institut des Hautes Études Scientifiques (IHES), France, for their kind hospitality during the course of the work. A.B thanks the participants of the BIRS-CMI workshop “Quantum Gravity and Information Theory: Modern Developments” (<https://www.birs.ca/events/2025/5-day-workshops/25w5386>) held at CMI, Chennai, during 9-14th November 2025 where part of the work was presented by J.S. J.S would like to thank the organizers of the BIRS-CMI workshop 2025 for giving warm hospitality. J.S is supported by the project CRG/2023/001120 and OTH/SERB/13451 (50:50 Postdoctoral scheme of IIT Gandhinagar). A.B is supported by the Core Research Grant (CRG/2023/001120) from the Anusandhan National Research Foundation, India. A.B also acknowledges the associateship program of the Indian Academy of Science, Bengaluru.

## A Another non-unitary minimal model $\mathcal{M}(7, 2)$

Very recently, there has been growing interest in the minimal model  $\mathcal{M}(7, 2)$  in the context of RG flows and non-invertible symmetries [97, 159–161].  $\mathcal{M}(7, 2)$  is a diagonal non-unitary Virasoro minimal model with central charge  $c = -\frac{68}{7}$  and non-vanishing conformal weights are  $\{-\frac{2}{7}, -\frac{3}{7}\}$ . It has three Virasoro primaries with non-trivial fusion

$$\Phi_2 \times \Phi_2 = \Phi_1 + \Phi_3, \tag{A.1}$$

$$\Phi_2 \times \Phi_3 = \Phi_2 + \Phi_3, \tag{A.2}$$

$$\Phi_3 \times \Phi_3 = \Phi_1 + \Phi_2 + \Phi_3. \tag{A.3}$$

Correspondingly, there are three Verlinde lines (defect lines) namely,  $\mathcal{L}_{\Phi_1}$ ,  $\mathcal{L}_{\Phi_2}$ , and  $\mathcal{L}_{\Phi_3}$  with quantum dimensions  $1, \frac{\cos \frac{3\pi}{14}}{\sin \frac{\pi}{7}}, \frac{1}{2\sin \frac{\pi}{14}}$  respectively and three Cardy boundary states  $|\Phi_1\rangle, |\Phi_2\rangle, |\Phi_3\rangle$ . The action of the defect lines on the primaries is given in the Table (8).

Defect line	$\Phi_1$	$\Phi_2$	$\Phi_3$
$\mathcal{L}_{\Phi_1}$	1	1	1
$\mathcal{L}_{\Phi_2}$	$-2 \sin \frac{3\pi}{14}$	$2 \sin \frac{\pi}{14}$	$\frac{\cos \frac{3\pi}{14}}{\sin \frac{\pi}{7}}$
$\mathcal{L}_{\Phi_3}$	$\frac{\sin \frac{\pi}{7}}{\cos \frac{3\pi}{14}}$	$-\frac{1}{2 \sin \frac{3\pi}{14}}$	$\frac{1}{2 \sin \frac{\pi}{14}}$

**Table 8:** Action of the  $\text{psu}(2)_5$  category on the primaries of  $\mathcal{M}(7, 2)$ .

It turns out that the Cardy boundary state  $|\Phi_3\rangle$  is a weakly symmetric under the above fusion category, known as  $\text{psu}(2)_5$  (It is a self-dual, multiplicity-free fusion category). This Cardy boundary state in terms of Ishibashi states is given by

$$|\Phi_3\rangle = \frac{\sqrt{2}}{7^{1/4}} \frac{\sin \frac{\pi}{7}}{\sqrt{\cos \frac{3\pi}{14}}} |\Phi_1\rangle - \frac{i\sqrt{2}}{7^{1/4}} \frac{\cos \frac{3\pi}{14}}{\sqrt{\cos \frac{\pi}{14}}} |\Phi_2\rangle + \frac{\sqrt{2}}{7^{1/4}} \frac{\cos \frac{\pi}{14}}{\sqrt{\sin \frac{\pi}{7}}} |\Phi_3\rangle. \quad (\text{A.4})$$

The annulus partition function in the closed and open-string channels with boundary state  $|\Phi_3\rangle$  is given by

$$Z(q) = \langle\langle \Phi_3 | \tilde{q}^{L_0 - \frac{c}{24}} | \Phi_3 \rangle\rangle, \quad (\text{A.5})$$

$$= \chi_1(q) + \chi_2(q) + \chi_3(q). \quad (\text{A.6})$$

From the action of the defect lines on the primaries listed in Table (8), we can write the resolved-partition function in the three sectors, namely,

$$Z(\mathcal{R}_1, q^n) = \frac{\chi_1(q^n)}{(Z(q))^n}, \quad (\text{A.7})$$

$$Z(\mathcal{R}_2, q^n) = \frac{\chi_2(q^n)}{(Z(q))^n}, \quad (\text{A.8})$$

$$Z(\mathcal{R}_3, q^n) = \frac{\chi_3(q^n)}{(Z(q))^n}. \quad (\text{A.9})$$

$\mathcal{M}(7, 2)$  is a non-unitary rational CFT; therefore, the leading contribution comes from the ground state rather than the vacuum. In this example,  $|\Omega\rangle = |\Phi_3\rangle$  is a ground state. Therefore, the symmetry-resolved  $n$ th Rényi entropy is

$$S_n(\mathcal{R}_1) = \frac{c_{\text{eff}}}{6} \left( \frac{n+1}{n} \right) \log \left( \frac{L}{\epsilon} \right) + \log \frac{2 \sin \frac{\pi}{7}}{\sqrt{7}} + \dots \quad (\text{A.10})$$

where the constant term

$$\log \frac{2 \sin \frac{\pi}{7}}{\sqrt{7}} = \log \left( \frac{d_{\mathcal{R}_1}}{\sum_{\mathcal{R}_i} d_{\mathcal{R}_i}} \right) + \log(\langle\langle \Phi_3 | \Omega \rangle\rangle \langle \Omega | \Phi_3 \rangle). \quad (\text{A.11})$$

where,  $d_{\mathcal{R}_1} = 1$ ,  $\sum_{\mathcal{R}_i} d_{\mathcal{R}_i} = 1 + \frac{\cos \frac{3\pi}{14}}{\sin \frac{\pi}{7}} + \frac{1}{2 \sin \frac{\pi}{14}} \sim 5.049$ , and  $\log(\langle\langle \Phi_3 \| \Omega \rangle\langle \Omega \| \Phi_3 \rangle\rangle) = \log\left(\frac{2}{\sqrt{7}} \frac{\cos^2 \frac{\pi}{14}}{\sin \frac{\pi}{7}}\right) \sim 0.504$  corresponds to the Affleck-Ludwig boundary entropy [133]. Similarly, for the other two sectors

$$S_n(\mathcal{R}_2) = \frac{c_{\text{eff}}}{6} \left(\frac{n+1}{n}\right) \log\left(\frac{L}{\epsilon}\right) + \log \frac{2 \cos \frac{3\pi}{14}}{\sqrt{7}} + \dots \quad (\text{A.12})$$

$$S_n(\mathcal{R}_3) = \frac{c_{\text{eff}}}{6} \left(\frac{n+1}{n}\right) \log\left(\frac{L}{\epsilon}\right) + \log \frac{2 \cos \frac{\pi}{14}}{\sqrt{7}} + \dots \quad (\text{A.13})$$

$$(\text{A.14})$$

and the constant terms are given by

$$\log \frac{2 \cos \frac{3\pi}{14}}{\sqrt{7}} = \log \left( \frac{d_{\mathcal{R}_2}}{\sum_{\mathcal{R}_i} d_{\mathcal{R}_i}} \right) + \log(\langle\langle \Phi_3 \| \Omega \rangle\langle \Omega \| \Phi_3 \rangle\rangle), \quad (\text{A.15})$$

$$\log \frac{2 \cos \frac{\pi}{14}}{\sqrt{7}} = \log \left( \frac{d_{\mathcal{R}_3}}{\sum_{\mathcal{R}_i} d_{\mathcal{R}_i}} \right) + \log(\langle\langle \Phi_3 \| \Omega \rangle\langle \Omega \| \Phi_3 \rangle\rangle) \quad (\text{A.16})$$

where,  $d_{\mathcal{R}_2} = \frac{\cos \frac{3\pi}{14}}{\sin \frac{\pi}{7}} \sim 1.802$ ,  $d_{\mathcal{R}_3} = \frac{1}{2 \sin \frac{\pi}{14}} \sim 2.247$ .

## References

- [1] Y. Choi, B. C. Raychaudhuri and Y. Zheng, *Noninvertible symmetry-resolved affleck-ludwig-cardy formula and entanglement entropy from the boundary tube algebra*, *Phys. Rev. Lett.* **133** (2024) 251602, [2409.02806].
- [2] E. P. Wigner, *Group Theory and Its Application to the Quantum Mechanics of Atomic Spectra*. Academic Press, New York, 1959.
- [3] D. Gaiotto, A. Kapustin, N. Seiberg and B. Willett, *Generalized global symmetries*, *JHEP* **02** (2015) 172, [1412.5148].
- [4] J. McGreevy, *Generalized Symmetries in Condensed Matter*, *Ann. Rev. Condensed Matter Phys.* **14** (2023) 57–82, [2204.03045].
- [5] L. Bhardwaj and Y. Tachikawa, *On finite symmetries and their gauging in two dimensions*, *JHEP* **03** (2018) 189, [1704.02330].
- [6] C.-M. Chang, Y.-H. Lin, S.-H. Shao, Y. Wang and X. Yin, *Topological Defect Lines and Renormalization Group Flows in Two Dimensions*, *JHEP* **01** (2019) 026, [1802.04445].
- [7] R. Thorngren and Y. Wang, *Fusion category symmetry. Part I. Anomaly in-flow and gapped phases*, *JHEP* **04** (2024) 132, [1912.02817].
- [8] B. Heidenreich, J. McNamara, M. Montero, M. Reece, T. Rudelius and I. Valenzuela, *Non-invertible global symmetries and completeness of the spectrum*, *JHEP* **09** (2021) 203, [2104.07036].

- [9] R. Thorngren and Y. Wang, *Fusion category symmetry. Part II. Categoriosities at  $c = 1$  and beyond*, *JHEP* **07** (2024) 051, [[2106.12577](#)].
- [10] Y. Choi, H. T. Lam and S. H. Shao, *Noninvertible global symmetries in the standard model*, *Phys. Rev. Lett.* **129** (2022) 161601, [[2205.05086](#)].
- [11] I. García Etzebarria, *Branes and Non-Invertible Symmetries*, *Fortsch. Phys.* **70** (2022) 2200154, [[2208.07508](#)].
- [12] C. Cordova and K. Ohmori, *Noninvertible Chiral Symmetry and Exponential Hierarchies*, *Phys. Rev. X* **13** (2023) 011034, [[2205.06243](#)].
- [13] C. Cordova, T. T. Dumitrescu, K. Intriligator and S.-H. Shao, *Snowmass White Paper: Generalized Symmetries in Quantum Field Theory and Beyond*, in *Snowmass 2021*, 5, 2022. [2205.09545](#).
- [14] Y. Choi, H. T. Lam and S.-H. Shao, *Non-invertible Gauss law and axions*, *JHEP* **09** (2023) 067, [[2212.04499](#)].
- [15] Y. Choi, H. T. Lam and S.-H. Shao, *Noninvertible Time-Reversal Symmetry*, *Phys. Rev. Lett.* **130** (2023) 131602, [[2208.04331](#)].
- [16] F. Apruzzi, I. Bah, F. Bonetti and S. Schafer-Nameki, *Noninvertible Symmetries from Holography and Branes*, *Phys. Rev. Lett.* **130** (2023) 121601, [[2208.07373](#)].
- [17] S.-H. Shao, *What's Done Cannot Be Undone: TASI Lectures on Non-Invertible Symmetries*, in *Theoretical Advanced Study Institute in Elementary Particle Physics 2023: Aspects of Symmetry*, 8, 2023. [2308.00747](#).
- [18] N. Seiberg and S.-H. Shao, *Majorana chain and Ising model - (non-invertible) translations, anomalies, and emanant symmetries*, *SciPost Phys.* **16** (2024) 064, [[2307.02534](#)].
- [19] S. Schafer-Nameki, *ICTP lectures on (non-)invertible generalized symmetries*, *Phys. Rept.* **1063** (2024) 1–55, [[2305.18296](#)].
- [20] L. Bhardwaj and S. Schafer-Nameki, *Generalized charges, part I: Invertible symmetries and higher representations*, *SciPost Phys.* **16** (2024) 093, [[2304.02660](#)].
- [21] L. Bhardwaj and S. Schafer-Nameki, *Generalized charges, part II: Non-invertible symmetries and the symmetry TFT*, *SciPost Phys.* **19** (2025) 098, [[2305.17159](#)].
- [22] L. Bhardwaj, L. E. Bottini, D. Pajer and S. Schafer-Nameki, *Categorical Landau Paradigm for Gapped Phases*, *Phys. Rev. Lett.* **133** (2024) 161601, [[2310.03786](#)].
- [23] Y. Choi, M. Forsslund, H. T. Lam and S.-H. Shao, *Quantization of Axion-Gauge Couplings and Noninvertible Higher Symmetries*, *Phys. Rev. Lett.* **132** (2024) 121601, [[2309.03937](#)].
- [24] Y.-H. Lin and S.-H. Shao, *Bootstrapping noninvertible symmetries*, *Phys. Rev. D* **107** (2023) 125025, [[2302.13900](#)].
- [25] N. Iqbal, *Jena lectures on generalized global symmetries: principles and applications*, 7, 2024. [2407.20815](#).
- [26] Y. Choi, Y. Sanghavi, S.-H. Shao and Y. Zheng, *Non-invertible and higher-form symmetries in  $2+1d$  lattice gauge theories*, *SciPost Phys.* **18** (2025) 008, [[2405.13105](#)].

- [27] N. Seiberg, S. Seifnashri and S.-H. Shao, *Non-invertible symmetries and LSM-type constraints on a tensor product Hilbert space*, *SciPost Phys.* **16** (2024) 154, [[2401.12281](#)].
- [28] L. Bhardwaj, L. E. Bottini, S. Schafer-Nameki and A. Tiwari, *Illustrating the categorical Landau paradigm in lattice models*, *Phys. Rev. B* **111** (2025) 054432, [[2405.05302](#)].
- [29] L. Bhardwaj, L. E. Bottini, S. Schafer-Nameki and A. Tiwari, *Lattice Models for Phases and Transitions with Non-Invertible Symmetries*, [2405.05964](#).
- [30] P. Putrov and R. Radhakrishnan, *Non-anomalous non-invertible symmetries in 1+1D from gapped boundaries of SymTFTs*, [2405.04619](#).
- [31] S.-H. Shao, J. Sorce and M. Srivastava, *Additivity, Haag duality, and non-invertible symmetries*, *JHEP* **08** (2025) 009, [[2503.20863](#)].
- [32] S.-H. Shao and S. Zhong, *Where Non-Invertible Symmetries End: Twist Defects for Electromagnetic Duality*, [2509.21279](#).
- [33] T. Bartsch, M. Bullimore and A. Grigoletto, *Representation theory for categorical symmetries*, [2305.17165](#).
- [34] D. Costa et al., *Simons Lectures on Categorical Symmetries*, 11, 2024. [2411.09082](#).
- [35] J. Preskill, *Quantum information and physics: some future directions*, *J. Mod. Opt.* **47** (2000) 127–137, [[quant-ph/9904022](#)].
- [36] A. Kitaev and J. Preskill, *Topological entanglement entropy*, *Phys. Rev. Lett.* **96** (2006) 110404, [[hep-th/0510092](#)].
- [37] A. Y. Kitaev, *Fault tolerant quantum computation by anyons*, *Annals Phys.* **303** (2003) 2–30, [[quant-ph/9707021](#)].
- [38] M. Levin and X.-G. Wen, *Detecting topological order in a ground state wave function*, *Phys. Rev. Lett.* **96** (Mar, 2006) 110405.
- [39] D. Aharonov, A. Kitaev and J. Preskill, *Fault-Tolerant Quantum Computation with Long-Range Correlated Noise*, *Phys. Rev. Lett.* **96** (2006) 050504, [[quant-ph/0510231](#)].
- [40] A. Feiguin, S. Trebst, A. W. W. Ludwig, M. Troyer, A. Kitaev, Z. Wang et al., *Interacting anyons in topological quantum liquids: The golden chain*, *Phys. Rev. Lett.* **98** (2007) 160409, [[cond-mat/0612341](#)].
- [41] E. Dennis, A. Kitaev, A. Landahl and J. Preskill, *Topological quantum memory*, *J. Math. Phys.* **43** (2002) 4452–4505, [[quant-ph/0110143](#)].
- [42] A. Di Meglio, K. Jansen, I. Tavernelli, C. Alexandrou, S. Arunachalam, C. W. Bauer et al., *Quantum computing for high-energy physics: State of the art and challenges*, *PRX Quantum* **5** (Aug, 2024) 037001.
- [43] M. Okada and Y. Tachikawa, *Noninvertible Symmetries Act Locally by Quantum Operations*, *Phys. Rev. Lett.* **133** (2024) 191602, [[2403.20062](#)].
- [44] L. Li, R.-Z. Huang and W. Cao, *Noninvertible symmetry-enriched quantum critical point*, *Phys. Rev. B* **112** (2025) L081113, [[2411.19034](#)].
- [45] Y. Fukusumi, *Fusion rule in conformal field theories and topological orders: A unified view of*

correspondence and (fractional) supersymmetry and their relation to topological holography, [2405.05178](#).

- [46] L. Bhardwaj, K. Inamura and A. Tiwari, *Fermionic non-invertible symmetries in (1+1)d: Gapped and gapless phases, transitions, and symmetry TFTs*, *SciPost Phys.* **18** (2025) 194, [[2405.09754](#)].
- [47] C. Feuchisin, N. Tantivasadakarn and V. V. Albert, *Noninvertible symmetry-protected topological order in a group-based cluster state*, *Phys. Rev. X* **15** (Mar, 2025) 011058.
- [48] Y. Li and A. Mitra, *Non-invertible symmetries out of equilibrium*, [2508.14213](#).
- [49] M. K. N. Balasubramanian, M. Buican, C. Delcamp and R. Radhakrishnan, *Gauging Non-Invertible Symmetries in (2+1)d Topological Orders*, [2507.01142](#).
- [50] A. Ocneanu, *Operator algebras, topology and subgroups of quantum symmetry – construction of subgroups of quantum groups –*, in *Taniguchi Conference on Mathematics Nara '98* (M. Maruyama and T. Sunada, eds.), vol. 31 of *Advanced Studies in Pure Mathematics*, pp. 235–263. Mathematical Society of Japan, 2001. [DOI](#).
- [51] M. Izumi, *The structure of sectors associated with longo–rehren inclusions: I. general theory*, *Communications in Mathematical Physics* **213** (2000) 127–179.
- [52] M. Mueger, *From Subfactors to Categories and Topology II. The quantum double of tensor categories and subfactors*, *arXiv Mathematics e-prints* (Nov., 2001) [math/0111205](#), [[math/0111205](#)].
- [53] M. Goldstein and E. Sela, *Symmetry-resolved entanglement in many-body systems*, *Phys. Rev. Lett.* **120** (2018) 200602, [[1711.09418](#)].
- [54] J. C. Xavier, F. C. Alcaraz and G. Sierra, *Equipartition of the entanglement entropy*, *Phys. Rev. B* **98** (2018) , [[1804.06357](#)].
- [55] A. Belin, L.-Y. Hung, A. Maloney, S. Matsuura, R. C. Myers and T. Sierens, *Holographic Charged Renyi Entropies*, *JHEP* **12** (2013) 059, [[1310.4180](#)].
- [56] R. Islam, R. Ma, P. M. Preiss, M. E. Tai, A. Lukin, M. Rispoli et al., *Measuring entanglement entropy through the interference of quantum many-body twins*, *Nature* **528** (2015) 77–83, [[1509.01160](#)].
- [57] A. Lukin, M. Rispoli, R. Schittko, M. E. Tai, A. M. Kaufman, S. Choi et al., *Probing entanglement in a many-body-localized system*, *Science* **364** (2019) 256–260, [<https://www.science.org/doi/pdf/10.1126/science.aau0818>].
- [58] N. Feldman and M. Goldstein, *Dynamics of Charge-Resolved Entanglement after a Local Quench*, *Phys. Rev. B* **100** (2019) 235146, [[1905.10749](#)].
- [59] S. Murciano, G. Di Giulio and P. Calabrese, *Symmetry resolved entanglement in gapped integrable systems: a corner transfer matrix approach*, *SciPost Phys.* **8** (2020) 046, [[1911.09588](#)].
- [60] S. Murciano, P. Ruggiero and P. Calabrese, *Symmetry resolved entanglement in two-dimensional systems via dimensional reduction*, *J. Stat. Mech.* **2008** (2020) 083102, [[2003.11453](#)].

- [61] G. Perez, R. Bonsignori and P. Calabrese, *Exact quench dynamics of symmetry resolved entanglement in a free fermion chain*, *J. Stat. Mech.* **2109** (2021) 093102, [[2106.13115](#)].
- [62] S. Murciano, G. Di Giulio and P. Calabrese, *Entanglement and symmetry resolution in two dimensional free quantum field theories*, *JHEP* **08** (2020) 073, [[2006.09069](#)].
- [63] S. Zhao, C. Northe and R. Meyer, *Symmetry-resolved entanglement in  $AdS_3/CFT_2$  coupled to  $U(1)$  Chern-Simons theory*, *JHEP* **07** (2021) 030, [[2012.11274](#)].
- [64] L. Capizzi, O. A. Castro-Alvaredo, C. De Fazio, M. Mazzoni and L. Santamaría-Sanz, *Symmetry resolved entanglement of excited states in quantum field theory. Part I. Free theories, twist fields and qubits*, *JHEP* **12** (2022) 127, [[2203.12556](#)].
- [65] D. X. Horvath, P. Calabrese and O. A. Castro-Alvaredo, *Branch Point Twist Field Form Factors in the sine-Gordon Model II: Composite Twist Fields and Symmetry Resolved Entanglement*, *SciPost Phys.* **12** (2022) 088, [[2105.13982](#)].
- [66] K. Weisenberger, S. Zhao, C. Northe and R. Meyer, *Symmetry-resolved entanglement for excited states and two entangling intervals in  $AdS_3/CFT_2$* , *JHEP* **12** (2021) 104, [[2108.09210](#)].
- [67] J. M. Magan, *Proof of the universal density of charged states in QFT*, *JHEP* **12** (2021) 100, [[2111.02418](#)].
- [68] F. Ares, P. Calabrese, G. Di Giulio and S. Murciano, *Multi-charged moments of two intervals in conformal field theory*, *JHEP* **09** (2022) 051, [[2206.01534](#)].
- [69] G. Di Giulio, R. Meyer, C. Northe, H. Scheppach and S. Zhao, *On the boundary conformal field theory approach to symmetry-resolved entanglement*, *SciPost Phys. Core* **6** (2023) 049, [[2212.09767](#)].
- [70] S. Zhao, C. Northe, K. Weisenberger and R. Meyer, *Charged moments in  $W_3$  higher spin holography*, *JHEP* **05** (2022) 166, [[2202.11111](#)].
- [71] H. Gaur and U. A. Yajnik, *Multi-charged moments and symmetry-resolved Rényi entropy of free compact boson for multiple disjoint intervals*, *JHEP* **01** (2024) 042, [[2310.14186](#)].
- [72] Y. Kusuki et al., *Symmetry-resolved entanglement entropy, spectra  $\mathcal{E}$  boundary conformal field theory*, *JHEP* **11** (2023) 216, [[2309.03287](#)].
- [73] C. Northe, *Entanglement Resolution with Respect to Conformal Symmetry*, *Phys. Rev. Lett.* **131** (2023) 151601, [[2303.07724](#)].
- [74] H. Gaur, *Total and Symmetry resolved Entanglement spectra in some Fermionic CFTs from the BCFT approach*, [2402.07557](#).
- [75] A. Banerjee et al., *Symmetry resolution in non-lorentzian field theories*, *JHEP* **06** (2024) 121, [[2404.02206](#)].
- [76] O. A. Castro-Alvaredo and L. Santamaría-Sanz, *Symmetry Resolved Measures in Quantum Field Theory: a Short Review*, [2403.06652](#).
- [77] H. Casini, M. Huerta, J. M. Magán and D. Pontello, *Entanglement entropy and superselection sectors. Part I. Global symmetries*, *JHEP* **02** (2020) 014, [[1905.10487](#)].
- [78] Y.-H. Lin, M. Okada, S. Seifnashri and Y. Tachikawa, *Asymptotic density of states in  $2d$  CFTs with non-invertible symmetries*, *JHEP* **03** (2023) 094, [[2208.05495](#)].

- [79] C. Copetti, L. Cordova and S. Komatsu, *S-matrix bootstrap and non-invertible symmetries*, *JHEP* **03** (2025) 204, [[2408.13132](#)].
- [80] S. Ali Ahmad, M. S. Klinger and Y. Wang, *The Many Faces of Non-invertible Symmetries*, [2509.18072](#).
- [81] P. Saura-Bastida, A. Das, G. Sierra and J. Molina-Vilaplana, *Categorical-symmetry resolved entanglement in conformal field theory*, *Phys. Rev. D* **109** (2024) 105026, [[2402.06322](#)].
- [82] V. Benedetti, H. Casini, Y. Kawahigashi, R. Longo and J. M. Magan, *Modular invariance as completeness*, *Phys. Rev. D* **110** (2024) 125004, [[2408.04011](#)].
- [83] A. Das, J. Molina-Vilaplana and P. Saura-Bastida, *Generalized symmetry resolution of entanglement in conformal field theory for twisted and anyonic sectors*, *Phys. Rev. D* **110** (2024) 125005, [[2409.02162](#)].
- [84] J. Heymann and T. Quella, *Revisiting the symmetry-resolved entanglement for noninvertible symmetries in 1+1d conformal field theories*, *Phys. Rev. D* **112** (2025) 025004, [[2409.02315](#)].
- [85] A. Das, J. Molina-Vilaplana and P. Saura-Bastida, *Entanglement, twist fields and anomalies for non-invertible symmetries*, *To appear* (2025) .
- [86] P. Calabrese and J. Cardy, *Entanglement entropy and conformal field theory*, *J. Phys. A* **42** (2009) 504005, [[0905.4013](#)].
- [87] J. Choi, B. C. Rayhaun, Y. Sanghavi and S.-H. Shao, *Remarks on boundaries, anomalies, and noninvertible symmetries*, *Phys. Rev. D* **108** (2023) 125005.
- [88] S. Seifnashri, S.-H. Shao and X. Yang, *Gauging non-invertible symmetries on the lattice*, *SciPost Phys.* **19** (2025) 063, [[2503.02925](#)].
- [89] P. Calabrese, J. Dubail and S. Murciano, *Symmetry-resolved entanglement entropy in Wess-Zumino-Witten models*, *JHEP* **10** (2021) 067, [[2106.15946](#)].
- [90] C. Northe, *Fermion Parity Resolution of Entanglement*, [2509.03605](#).
- [91] K. Ohmori and Y. Tachikawa, *Physics at the entangling surface*, *J. Stat. Mech.* **1504** (2015) P04010, [[1406.4167](#)].
- [92] J. Cardy and E. Tonni, *Entanglement hamiltonians in two-dimensional conformal field theory*, *Journal of Statistical Mechanics: Theory and Experiment* **2016** (dec, 2016) 123103.
- [93] Y. Choi, B. C. Rayhaun and Y. Zheng, *Generalized Tube Algebras, Symmetry-Resolved Partition Functions, and Twisted Boundary States*, [2409.02159](#).
- [94] E. M. Brehm and I. Runkel, *Lattice models from cft on surfaces with holes: I. torus partition function via two lattice cells*, *J. Phys. A* **55** (2022) 235001.
- [95] E. M. Brehm and I. Runkel, *Lattice models from cft on surfaces with holes ii: Cloaking boundary conditions and loop models*, [2410.19938](#).
- [96] M. Fossati, F. Ares and P. Calabrese, *Symmetry-resolved entanglement in critical non-Hermitian systems*, *Phys. Rev. B* **107** (2023) 205153, [[2303.05232](#)].
- [97] Y. Fukusumi and T. Kawamoto, *Generalizing quantum dimensions: Symmetry-based classification of local pseudo-Hermitian systems and the corresponding domain walls*, [2511.11059](#).

- [98] E. Witten, *Quantum Field Theory and the Jones Polynomial*, *Commun. Math. Phys.* **121** (1989) 351–399.
- [99] G. W. Moore and N. Seiberg, *Classical and Quantum Conformal Field Theory*, *Commun. Math. Phys.* **123** (1989) 177.
- [100] G. W. Moore and N. Seiberg, “Lectures on rcft.” RU-89-32, 1989.
- [101] R. Dijkgraaf and E. Witten, *Topological Gauge Theories and Group Cohomology*, *Commun. Math. Phys.* **129** (1990) 393.
- [102] E. P. Verlinde, *Fusion rules and modular transformations in 2d conformal field theory*, *Nucl. Phys. B* **300** (1988) 360–376.
- [103] J. Fuchs, I. Runkel and C. Schweigert, *Twenty-five years of two-dimensional rational conformal field theory*, *J. Math. Phys.* **51** (2010) 015210, [0910.3145].
- [104] D. Gang, H. Kim and S. Stubbs, *Three-Dimensional Topological Field Theories and Nonunitary Minimal Models*, *Phys. Rev. Lett.* **132** (2024) 131601, [2310.09080].
- [105] D. Gang, D. Kim and S. Lee, *A non-unitary bulk-boundary correspondence: Non-unitary haagerup rcfts from s-fold scfts*, *SciPost Phys.* **17** (2024) 064, [2310.14877].
- [106] D. Gang and D. Kim, *Generalized non-unitary Haagerup-Izumi modular data from 3D S-fold SCFTs*, *JHEP* **03** (2023) 185, [2211.13561].
- [107] U. Haagerup, *Principal graphs of subfactors in the index range  $4 < [m : n] < 3 + \sqrt{2}$* , Subfactors (Proceedings of Taniguchi Symposium, Kyuzeso, 1993) **1** (1994) 1–38.
- [108] D. E. Evans and T. Gannon, *The exoticness and realisability of twisted haagerup-izumi modular data*, *Commun. Math. Phys.* **307** (2011) 463–512, [1006.1326].
- [109] T. C. Huang, Y. H. Lin, K. Ohmori, Y. Tachikawa and M. Tezuka, *Numerical evidence for a haagerup conformal field theory*, *Phys. Rev. Lett.* **128** (2022) 231603, [2110.03008].
- [110] R. Vanhove et al., *Critical lattice model for a haagerup conformal field theory*, *Phys. Rev. Lett.* **128** (2022) 231602, [2110.03532].
- [111] Z. Jia, *Quantum cluster state model with haagerup fusion category symmetry*, *Advanced Quantum Technologies* (2025) e00305, [2412.19657].
- [112] L. E. Bottini and S. Schafer-Nameki, *Construction of a Gapless Phase with Haagerup Symmetry*, *Phys. Rev. Lett.* **134** (2025) 191602, [2410.19040].
- [113] T. Gannon, *Cft and modular forms*, *Workshop 25w5318: Recent Developments in Logarithmic Conformal Field Theory at BIRS, July 21, 2025* .
- [114] F. Benini, P. Calabrese, M. Fossati, A. H. Singh and M. Venuti, *Entanglement Asymmetry for Higher and Noninvertible Symmetries*, **2509.16311**.
- [115] P. Di Francesco, P. Mathieu and D. Senechal, *Conformal Field Theory*. Graduate Texts in Contemporary Physics. Springer-Verlag, New York, 1997, 10.1007/978-1-4612-2256-9.
- [116] R. Bonsignori and P. Calabrese, *Boundary effects on symmetry resolved entanglement*, *J. Phys. A* **54** (2021) 015005, [2009.08508].
- [117] N. Ishibashi, *The Boundary and Crosscap States in Conformal Field Theories*, *Mod. Phys. Lett. A* **4** (1989) 251.

- [118] J. L. Cardy, *Effect of boundary conditions on the operator content of two-dimensional conformally invariant theories*, *Nucl. Phys. B* **275** (1986) 200–218.
- [119] J. L. Cardy, *Boundary conditions, fusion rules and the verlinde formula*, *Nucl. Phys. B* **324** (1989) 581–596.
- [120] J. Cardy, *Boundary conditions in conformal field theory*, in *Adv. Stud. Pure Math.*, vol. 19, pp. 127–148, 1989.
- [121] J. L. Cardy and D. C. Lewellen, *Bulk and boundary operators in conformal field theory*, *Phys. Lett. B* **259** (1991) 274–278.
- [122] J. L. Cardy, *Boundary conformal field theory*, 2004.
- [123] C. Northe, *Young Researchers School 2024 Maynooth: lectures on CFT, BCFT and DCFT*, *J. Phys. A* **58** (2025) 103001, [[2411.03381](#)].
- [124] A. Recknagel and V. Schomerus, *Boundary Conformal Field Theory and the Worldsheet Approach to D-Branes*. Cambridge Monographs on Mathematical Physics. Cambridge University Press, 11, 2013, [10.1017/CBO9780511806476](#).
- [125] W. Donnelly and G. Wong, *Entanglement branes, modular flow, and extended topological quantum field theory*, *JHEP* **10** (2019) 016, [[1811.10785](#)].
- [126] L. Y. Hung and G. Wong, *Entanglement branes and factorization in conformal field theory*, *Phys. Rev. D* **104** (2021) 026012, [[1912.11201](#)].
- [127] R. Bonsignori, P. Ruggiero and P. Calabrese, *Symmetry resolved entanglement in free fermionic systems*, *J. Phys. A* **52** (2019) 475302, [[1907.02084](#)].
- [128] V. B. Petkova and J. B. Zuber, *Generalized twisted partition functions*, *Phys. Lett. B* **504** (2001) 157–164, [[hep-th/0011021](#)].
- [129] E. Ardonne and J. Slingerland, *Clebsch–gordan and 6j-coefficients for rank 2 quantum groups*, *Journal of Physics A: Mathematical and Theoretical* **43** (Aug., 2010) 395205.
- [130] G. Verceleyen and J. Slingerland, *On low rank fusion rings*, [2205.15637](#).
- [131] K. Graham and G. M. T. Watts, *Defect lines and boundary flows*, *JHEP* **04** (2004) 019, [[hep-th/0306167](#)].
- [132] Y. Fukusumi and S. Iino, *Open spin chain realization of a topological defect in a one-dimensional Ising model: Boundary and bulk symmetry*, *Phys. Rev. B* **104** (2021) 125418, [[2004.04415](#)].
- [133] I. Affleck and A. W. W. Ludwig, *Universal noninteger ‘ground state degeneracy’ in critical quantum systems*, *Phys. Rev. Lett.* **67** (1991) 161–164.
- [134] B. Haghighat and Y. Sun, *Topological Defect Lines in bosonized Parafermionic CFTs*, *Adv. Theor. Math. Phys.* **28** (2024) 1987–2023, [[2306.16555](#)].
- [135] R. E. Behrend, P. A. Pearce and J.-B. Zuber, *Integrable boundaries, conformal boundary conditions and A-D-E fusion rules*, *J. Phys. A* **31** (1998) L763–L770, [[hep-th/9807142](#)].
- [136] R. E. Behrend, P. A. Pearce, V. B. Petkova and J.-B. Zuber, *Boundary conditions in rational conformal field theories*, *Nucl. Phys. B* **570** (2000) 525–589, [[hep-th/9908036](#)].
- [137] T. J. Hagge and S.-M. Hong, *Some non-braided fusion categories of rank 3*, 2007.

- [138] I. Affleck, M. Oshikawa and H. Saleur, *Boundary critical phenomena in the three state Potts model*, *J. Phys. A* **31** (1998) 5827, [[cond-mat/9804117](#)].
- [139] M. Sinha, F. Yan, L. Grans-Samuelsson, A. Roy and H. Saleur, *Lattice realizations of topological defects in the critical (1+1)-d three-state Potts model*, *JHEP* **07** (2024) 225, [[2310.19703](#)].
- [140] X. Gu and X. Xie, *Generalized Cardy conditions of topological defect lines*, [2310.15487](#).
- [141] L. Capizzi, D. X. Horváth, P. Calabrese and O. A. Castro-Alvaredo, *Entanglement of the 3-state Potts model via form factor bootstrap: total and symmetry resolved entropies*, *JHEP* **05** (2022) 113, [[2108.10935](#)].
- [142] P. Bantay and T. Gannon, *Conformal characters and the modular representation*, *JHEP* **02** (2006) 005, [[hep-th/0512011](#)].
- [143] P. Bantay and T. Gannon, *Vector-valued modular functions for the modular group and the hypergeometric equation*, *Commun. Num. Theor. Phys.* **1** (2007) 651–680.
- [144] S. Govindarajan, A. Sadanandan and J. Santara, *Quasi-Characters for three-character Rational Conformal Field Theories*, [2510.24248](#).
- [145] S. Govindarajan and J. Santara, *Two approaches to the holomorphic modular bootstrap*, *JHEP* **10** (2025) 181, [[2503.23761](#)].
- [146] S. D. Mathur, S. Mukhi and A. Sen, *On the Classification of Rational Conformal Field Theories*, *Phys. Lett. B* **213** (1988) 303–308.
- [147] S. D. Mathur, S. Mukhi and A. Sen, *Reconstruction of Conformal Field Theories From Modular Geometry on the Torus*, *Nucl. Phys. B* **318** (1989) 483–540.
- [148] S. G. Naculich, *DIFFERENTIAL EQUATIONS FOR RATIONAL CONFORMAL CHARACTERS*, *Nucl. Phys. B* **323** (1989) 423–440.
- [149] H. R. Hampapura and S. Mukhi, *On 2d Conformal Field Theories with Two Characters*, *JHEP* **01** (2016) 005, [[1510.04478](#)].
- [150] A. Das, C. N. Gowdigere and J. Santara, *Classifying three-character RCFTs with Wronskian index equalling 0 or 2*, *JHEP* **11** (2021) 195, [[2108.01060](#)].
- [151] A. R. Chandra and S. Mukhi, *Towards a Classification of Two-Character Rational Conformal Field Theories*, *JHEP* **04** (2019) 153, [[1810.09472](#)].
- [152] L. Bhardwaj, D. Pajer, S. Schafer-Nameki, A. Tiwari, A. Warman and J. Wu, *Gapped phases in (2+1)d with non-invertible symmetries: Part I*, *SciPost Phys.* **19** (2025) 056, [[2408.05266](#)].
- [153] L. Bhardwaj, S. Schafer-Nameki, A. Tiwari and A. Warman, *Gapped Phases in (2+1)d with Non-Invertible Symmetries: Part II*, [2502.20440](#).
- [154] S. Schafer-Nameki, A. Tiwari, A. Warman and C. Zhang, *SymTFT Approach for Mixed States with Non-Invertible Symmetries*, [2507.05350](#).
- [155] I. García Etxebarria, J. Huertas and A. M. Uranga, *SymTFT Fans: The Symmetry Theory of 4d N=4 Super Yang-Mills on spaces with boundaries*, [2409.02156](#).
- [156] L. Bhardwaj, L. E. Bottini, D. Pajer and S. Schafer-Nameki, *The club sandwich: Gapless*

- phases and phase transitions with non-invertible symmetries*, *SciPost Phys.* **18** (2025) 156, [[2312.17322](#)].
- [157] F. Apruzzi, N. Dondi, I. García Etxebarria, H. T. Lam and S. Schafer-Nameki, *Symmetry TFTs for Continuous Spacetime Symmetries*, [2509.07965](#).
- [158] L. Bhardwaj, C. Copetti, D. Pajer and S. Schafer-Nameki, *Boundary SymTFT*, *SciPost Phys.* **19** (2025) 061, [[2409.02166](#)].
- [159] F. Ambrosino and S. Negro, *Minimal Model Renormalization Group Flows: Noninvertible Symmetries and Nonperturbative Description*, *Phys. Rev. Lett.* **135** (2025) 021602, [[2501.07511](#)].
- [160] A. Katsevich, I. R. Klebanov, Z. Sun and G. Tarnopolsky, *Towards a Quintic Ginzburg-Landau Description of the (2, 7) Minimal Model*, [2510.19085](#).
- [161] M. Blakeney, L. Corcoran, M. de Leeuw, B. Pozsgay and E. Vernier, *Temperley-Lieb integrable models and fusion categories*, [2510.19902](#).